CL-08
DEVULCANIZATION AS AN OPPORTUNITY TO RECYCLE RUBBER

MAREIKE HESS, HARALD GEISLER, and ROBERT H. SCHUSTER

German Institute for Rubber Technology e.V., Eupenerstraße 33, 30519 Hannovert
Mareike.Hess@DIKautschuk.de

How to reduce rubber waste? There are several options to reduce rubber waste. A well known method is to burn the rubber waste to produce energy while producing cement. This kind of "recycling" has to be reduced in future. Due to its irreversible network, the different compounds and ingredients the recycling of rubber is not comparable with the recycling of plastics. In most cases the methods of recycling show unsatisfactory results for reuse. The "recycled" rubber crumb is typically used as an inactive filler for simple undemanding products. The aim of this research project is to produce recycled rubber which can be used without any additional ingredients.

Introduction

Devulcanization provides an opportunity to recycle rubber. It is the opposite of vulcanization. Thus, it is a process, which opens di- and polysulfidic bonds of sulphur-vulcanized rubber. Due to their high bonding energy it is impossible decomposing monosulfidic bonds yet. Ideally, it is possible to reuse a completely devulcanized elastomer without any other additionals.

There are several processes to devulcanize: mechanical, chemical, mechanic-chemical, biological and with the help of microwaves or ultrasonic. The chosen mechanic-chemical method has the advantage of being highly efficient, rapid and technically applicable.

The effectiveness of the devulcanizing chemicals is first investigated using squalene as a model compound, to replace polyisoprene rubber. Afterwards the chosen promising chemicals are tested in mechanic-chemical devulcanization of sulphur vulcanized polyisoprene rubber.

The mechanism of devulcanization of sulphur-vulcanized polyisoprene rubber with amines or disulphides can occur radical[1−3]or ionic[4].

After devulcanization the devulcanized rubber or mixtures which contain devulcanized rubber can be revulcanized. Physical properties of revulcanizates are measured and compared with those of the start-vulcanizates.

Experimental

The first step is to find a devulcanizing agent. Therefore networking and depolymerisation were accomplished with a model molecule used to mimick polyisoprene rubber. These molecules e.g. squalene

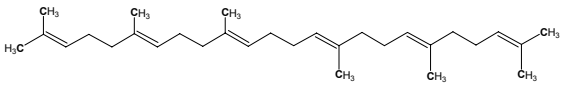

have a lower moleculare mass. Because of this attribute the substances are liquid and thus much easier to handle and analyse. With the aid of sulfur and an accelerator squalene was crosslinked. The curing in an autoclave (Fig. 1) took 60 minutes at 150 °C under nitrogen atmosphere and continuos stirring. The desulfuration was carried out through adding equimolare masses of different devulcanizing agents and again stirring for 60 minutes at 150 °C.

The best desulfurating agents were chosen to accomplish the rubber recycling by the mechanic-chemical method of devulcanization. Vulcanizated polyisoprene rubber was recycled using the internal mixer shown in Fig. 2 adding so-called devulcanizing agents.

Therefore the vulcanizate was reduced into small pieces. The internal mixer was filled with the rubber crumbs and the

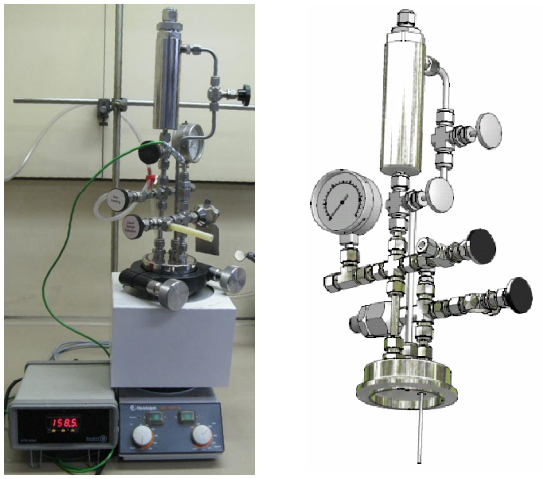

Fig. 1. **Autoclave, used to accomplish the model networking and desulfuration**

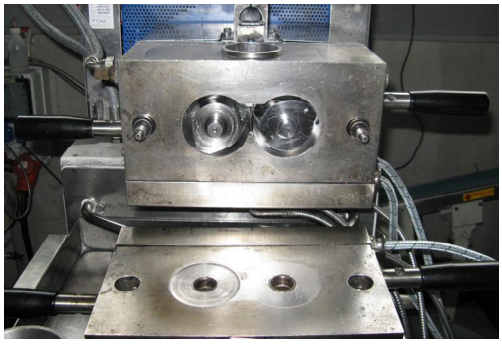

Fig. 2. **Internal mixer, used to accomplish the mechanic-chemical method of devulcanization**

devulcanizing agent. Through variation of temperature, mixing time, rotation speed, concentration of the devulcanizing agent, particle size and filling degree the rubber was going to be devulcanized[5].

Analytics and Results

During curing and desulfuration in the autoclave samples were taken to measure the distribution of their molar mass by GPC. Ideally after cross-linking the samples have multiple masses of squalene and after desulfuration again the mass of only one molecule of squalene. Fig. 3 shows the distribution of molar mass measured by GPC and with it the efficiency of different tested desulfuration agents.

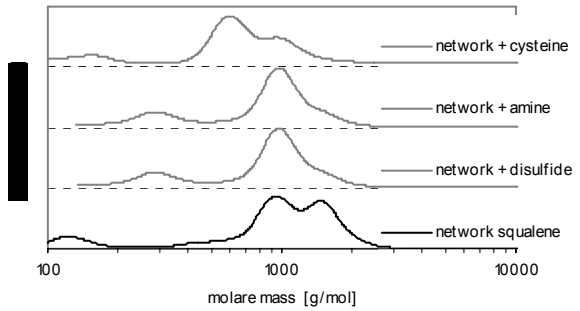

Fig. 3. **Distribution of molar mass measured by GPC to show the efficiency of different desulfuration agents**

Before desulfuration the samples had two, three and four times the molecular mass of squalene. After devulcanization with an amine or disulfide their molecular masses counted the twice mass of squalene. With the help of a cysteine the molecular mass of the desulfuration product almost had the molecular mass of only one molecule of squalene.

To compare the effectiveness of the three chemicals the following devulcanization experiments were done using these three chemicals.

After devulcanization in the internal mixer the viscosities of all samples were checked. To optimize the procedure the results are compared with the viscosity of the original polymer and the pure mechanical devulcanizates as can be seen in Fig. 4.

With the aid of IR measurements it was possible to confirm the preservation of the double bond character.

Furthermore GPC measurements followed to get informations about the distribution of the molar mass and with it also about the efficiency of tested devulcanizing agents.

Promising samples were mixed in different parts with the respective fresh polymer. Cross-linking agents were added and the mixtures were revulcanized. Their revulcanizing properties as well as their physical properties, i.e. stress-strain measurements, were measured and compared with the datas of the respective original vulcanizate.

In Fig. 5 the results of measuring the hardness Shore A and the swelling degree of the revulcanizates are shown. If the hardness is lower, the swelling degree increases because the

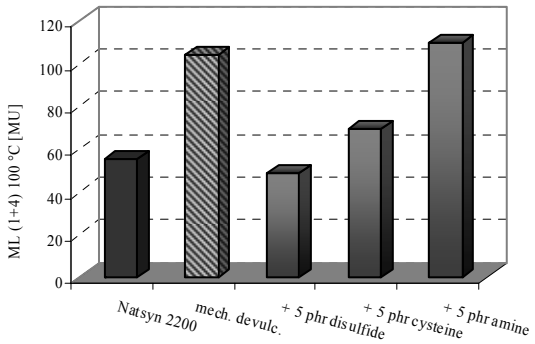

Fig. 4. **Mooney Viscosity after devulcanization at 150 °C in the internal mixer**

network density is lower as well. The results are compared with the original vulcanizate. The properties do not differ that much. Only the revulcanizate which contains devulcanizate decomposed with the help of a disulfide didn`t achieve the same properties.

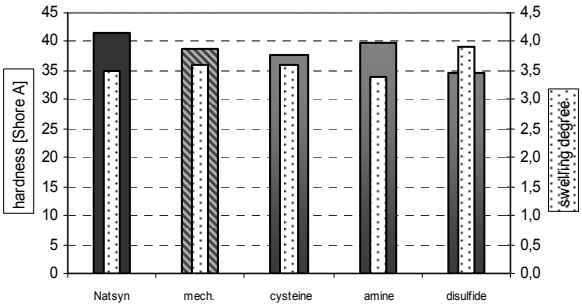

Fig. 5. **Hardness Shore A and swelling degree of some revulcanizates in comparison with the start-vulcanizate**

Stress-strain curves are graphical representations of the correlation between stress, derived from measuring the load applied on the sample, and strain, derived from measuring the deformation of the sample. The following diagram illustrates the stress-strain behaviour of the original vulcanizate and the revulcanizates.

Comparing the properties of the revulcanizates with the original vulcanizate and with it the effectiveness of the devulcanization and followed revulcanization, the use of a cysteine as a devulcanizing agent shows the best results. The following TEM pictures were used to see the distribution of the cysteindevulcanizate and the fresh polymer in the revulcanizate. To be able to distinguish between fresh polymer and devulcanizate, two phr carbon black were added the fresh polymer before mixing with the devulcanizate. The carbon black agglomerates show the parts with fresh polymer and the brighter parts with darker pieces inside show domains with cystein-

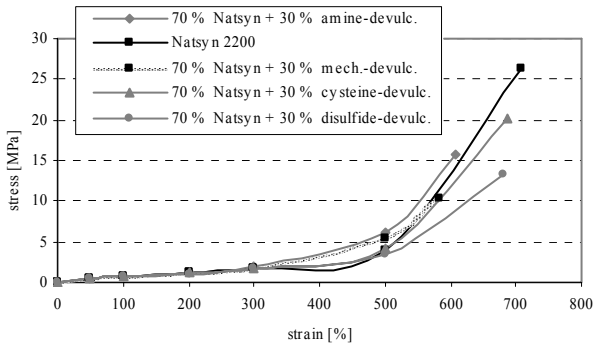

Fig. 6. **Stress-strain measurements of some selected revulcanizates what contain 30 % of different devulcanizates**

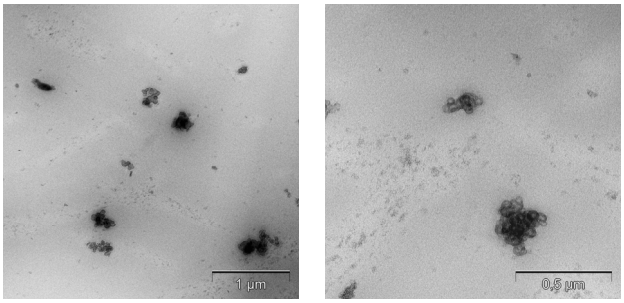

Fig. 7. **Transmission-Electron-Microscope (TEM) pictures of a revulcanizate which contains 30 % of cysteine-devulcanizate**

devulcanizate. The size of the domains are about one micrometer indicating a good intermixture.

Conclusions

Doing desulfuration measurements in an autoclave is a good opportunity to find out which chemicals are able to decompose a sulfur network and with it sulfidic bonds. Mechanic-chemical devulcanization is more effective than mechanical devulcanization. Revulcanizates including 30 % devulcanizate and 70 % polymere show promising results in physical properties.

Outlook

Ideally it will be possible to find out the mechanism of desulfuration and with it also the mechanism of devulcanization. Therefore it will be important to find out which products instead of the de-cross-linked network are produced during desulfuration / devulcanization. Furthermore it will be possible to clarify the kind of sulfidic bonds not only in (re-) vulcanizates by thiol-amine-methode also in liquid model-networks. Therefore de-cross-linked and re-cross-linked model molecules have to be analysed by means of NMR, HPLC[6], GCMS, IR and further GPC measurements.

The financial support of Schill & Seilacher, Oerlikon Accotex Texparts, Gummiwerk Kraiburg and Ellerbrock Runderneuerung is acknowledged.

REFERENCES

1. Kende I., Pickering T. L., Tobolsky A. V.: J. Am. Chem. Soc. *87*, 5582 (1965).
2. Pickering T. L., Saunders K. L., Tobolsky A. V.: J. Am. Chem. Soc. *89*, 2364 (1967).
3. Pickering T. L., Saunders K. J., Tobolsky A. V., in: *The Chemistry of Sulphides*, (Tobolsky A. V., ed.). pp 61. Interscience Publishers, New York 1968.
4. Milligan B.: Rubber Chem. Technol. *39*, 1115 (1966).
5. Kohler R., O, Neill J.: GAK *51*, 432 (1998).
6. Dierkes W., Rajan V., Noordermeer J. W. M.: KGK *58*, 312 (2005).

CL-09
IMPROVEMENT OF MECHANICAL AND TERMOMECHANICAL PROPERTIES OF POLYETHYLENE BY IRRADIATION CROSSLINKING

ZDENEK HOLIK[a], MIROSLAV MANAS[b], MICHAL DANEK[c], and JIŘÍ MACOUREK[a]

[a] Tomas Bata University in Zlin, Faculty of Technology, Department of Production Engineering, TGM 275, 762 72 Zlin, Czech Republic, [b] Tomas Bata University in Zlin, Faculty of Technology, Department of Production Engineering, TGM 275, 762 72 Zlin, Czech Republic, [c] BGS Beta – Gamma GmbH & Co.KG. – Service, Wiehl, Germany
holik@ft.utb.cz, manas@ft.utb.cz, danek@bgs.eu,

Abstract

The main objective of the study is investigation of mechanical and termomechanical properties of polyethylene. These properties were examined in dependence on the dosage of the ionizing electron beam (beta) radiation. Non-irradiated samples and those irradiated by dosage 15, 30, 45, 66, 99, 132, 165 and 198 kGy were compared.

Radiation cross-linking of polyolefin's results in increased mechanical strength, heat resistance, and breakdown voltage, and improved insulation properties, particularly at high temperatures.

Introduction

Radiation modification of materials refers to the production of beneficial changes by exposure to radiation. High-energy (ionizing) radiation is used most often to modify polymers. Irradiation crosslinking is the one of possible method how to get the required quality and it is a process

whereat it can be optimised properties of standard or engineering polymers and impart to them mechanical, thermal and chemical properties of high performance polymers. The main group presents standard polymers and it is the most considerable one and it is share in the production of all polymers is as high as 90 %. The engineering polymers offers much better properties in comparison with standard polymers. The production of these types of polymers takes less than 10 %. High performance polymers have the best mechanical and thermal properties but the share in production and use of all polymers is less than 1 %.

The most common forms of radiation employed are electromagnetic (gamma) radiation from the radioisotopes cobalt-60 and celsium-137, and electron beams (beta) generated by electron accelerators. Radiation processing covers use those beta or gamma radiations to break up bonds between atoms. Consequently, free radicals rise in materials that react with one another during chemical reactions (Fig. 1). The main difference between beta and gamma rays lies in their abilities of penetrating the irradiated material. Gamma rays have a high penetration capacity. The penetration capacity of electron rays depends on the energy of the accelerated electrons (Fig. 2 and Fig. 3)[1].

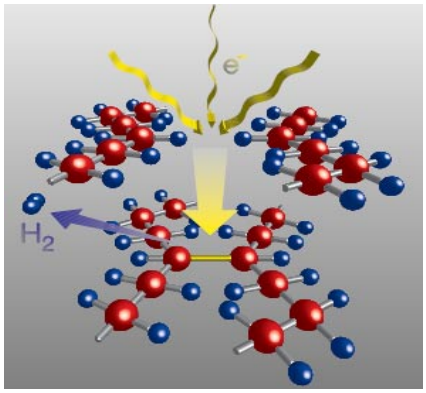

Fig. 1. **Scheme of irradiation crosslinking[2]**

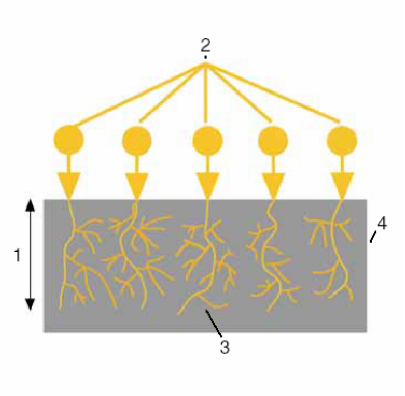

Fig. 2. **Design of Electron rays[2],** 1 – penetration depth of electron, 2 – primary electron, 3 – secondary electron, 4 – irradiated material

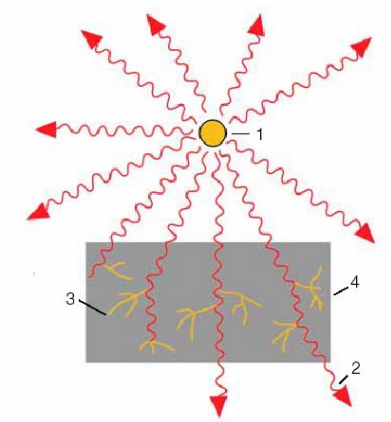

Fig. 3. **Design of Gamma rays[2],** 1 – encapsulated Co – 60 radiation source, 2 – Gamma ray 3 – secondary electrons, 4 – irradiated material

Experiment

The samples were prepared on the injection moulding machine (ARBURG ALLROUNDER 420 C 1000-350).

The materials of the all samples were polyethylene (PE), provided by The Dow Chemical Company:

- DOW HDPE 25055 E
- DOW LDPE 780 E

Processing conditions during the injection moulding were according to the recommendation of the producers.

All samples were irradiated with electron rays (electron energy 10 MeV, dosis: 15, 33, 45, 66, 99, 132, 165 and 198 kGy) in the firm BGS Beta Gamma Service GmbH & Co, Saal am Donau – Germany.

The following tests were carried out and equipment used:

- Tensile test, according to standard CSN EN ISO 527-1, 527-2 were carried out on tensile machine ZWICK 1456. Used rate: LDPE – 50 mm min^{-1}; HDPE – 50 mm min^{-1}. Test data was processed by Test Xpert Standard software and modulus (E [MPa]), tensile stress (σ_t [MPa]) were determined.
- TMA test (Thermal mechanical analysis) was carried out on Perkin – Elmer Thermal.

Results

Comparison of tensile strength and E – modulus (at 23 °C) of high-density polyethylene (HDPE) and low-density polyethylene (LDPE) before and after irradiation is given in the Fig. 3 and Fig. 4. It is evident that crosslinking improves the tensile strength (σ_t) and E – modulus of both PE.

The irradiation has a positive effect on tensile strength (σ_t) – both irradiated polyethylenes have reached higher value of tensile strength than non-irradiated polyethylene. After irradiation it is higher nearly by 10 % in case of LDPE and by 5 % in case of HDPE. However, as can be seen from Fig. 3, the highest value of doses does not mean a highest value of tensile strength.

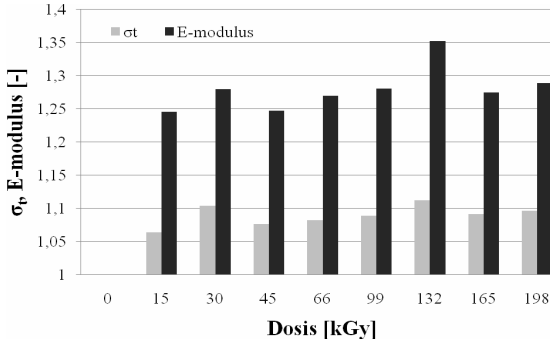

Fig. 3. **Comparisons of tensile strength and E – modulus of LDPE – 23 °C**

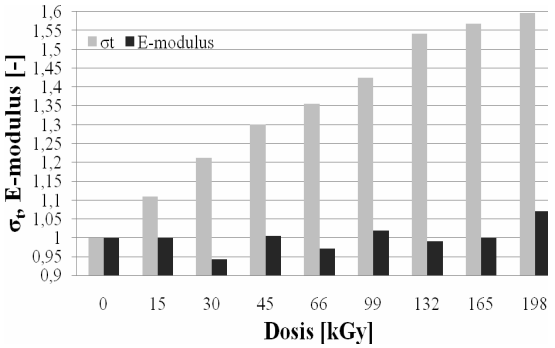

Fig. 5. **Comparisons of tensile strength and E – modulus of LDPE – 100 °C**

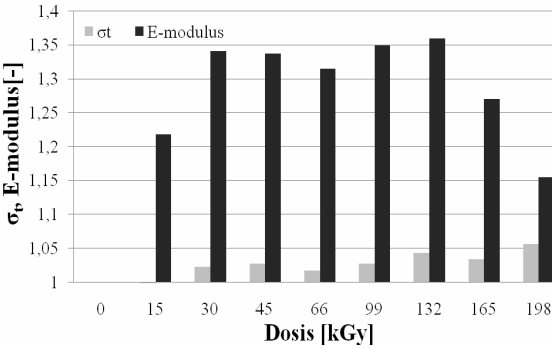

Fig. 4. **Comparisons of tensile strength and E – modulus of HDPE – 23 °C**

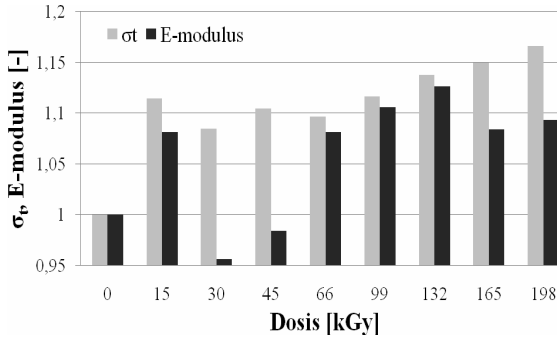

Fig. 6. **Comparisons of tensile strength and E – modulus of HDPE – 100 °C**

The irradiation has also a positive effect on E-modulus of both polyethylenes. After irradiation it is higher nearly by 30–35 % in case of LDPE and by 35 % in case of HDPE.

A positive effect of irradiation on tensile strength is much higher at 100 °C than at 23 °C but for LDPE only. After irradiation it is higher nearly by 60 % in case of LDPE irradiated by doses 198 kGy and by 10 % in case of HDPE. On the other hand, E – modulus does not increase significantly in case of both polyethylenes.

Finally, thermal stability of both irradiated polyethylenes increases with dosages. Fig. 7 and 8 show the thermal stability given as the position of a probe of irradiated LDPE and HDPE. The graph has eight curves. Each curve represents one dosage. The graph shows that the thermal stability of irradi-

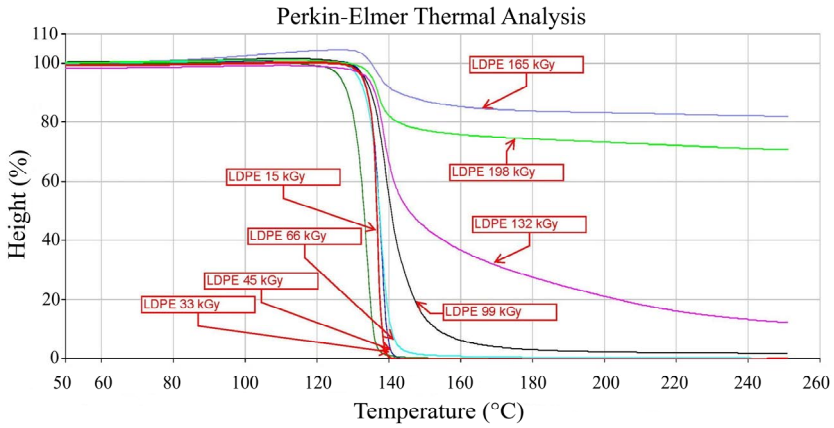

Fig. 7. **Results of thermal stability of LDPE**

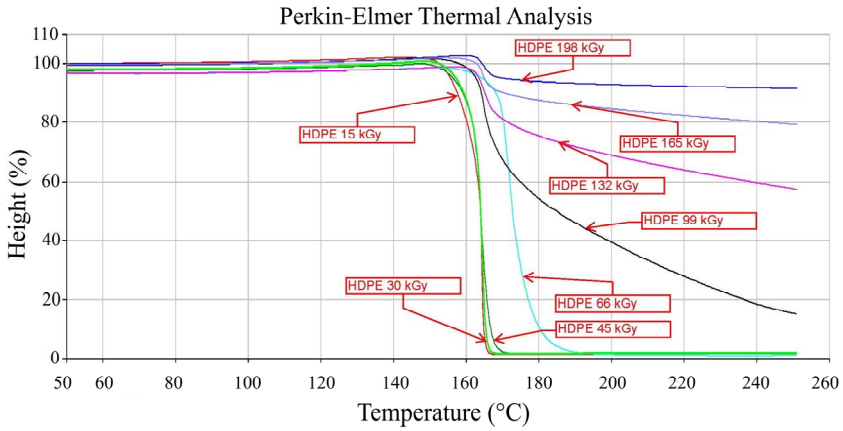

Fig. 8. **Results of thermal stability of HDPE**

ated LDPE (in case of dosage 165 kGy) and HDPE (in case of 198 kGy) are thermally stable up to 250 °C.

Conclusion

From the results of tests it is evident, that irradiation crosslinking improve the mechanical properties of each polyethylene. The improvement is more considerable in case of higher temperature (100 °C), in addition LDPE and HDPE show the greatest changes in thermomechanical properties.

That is a consequence of creation of cross-link (during irradiation crosslinking) and protraction of macromolecular string, which is than more flexible during thermal load than shorter macromolecular strings.

This article is financially supported by the Czech Ministry of Education, Youth and Sports in th R&D project under the title of 'Modelling and Control of Processing Procedures of Natural and Synthetic Polymers', No. MSM 7088352102.

REFERENCES

1. Woods R. J.: *Applied Radiation Chemistry: Radiation Processing*, 1994, ISBN 0-471-54452-3.
2. http://www.bgs.com/
3. http://www.pts-marketing.de/
4. Mańas D.: Improvement of Plastic Properties, Inter. Sci. J., www.archivesmse.org

CL-10

ARAMID REINFORCEMENT FOR LOW WEIGHT, LONG SERVICE LIFE AND FUEL SAVING

GERARD VAN DEN HONDEL

Elastomer Reinforcements, Teijin Aramid BV, Westervoortsedijk 73, NL-6827 AV Arnhem gerard.vandenhondel@teijinaramid.com

The automotive industry grew very rapidly in Central Europe, leading to large supply opportunities for local rubber parts producers. Aramids are para-crystalline materials for yarns with very high strength to weight ratio (tenacity):

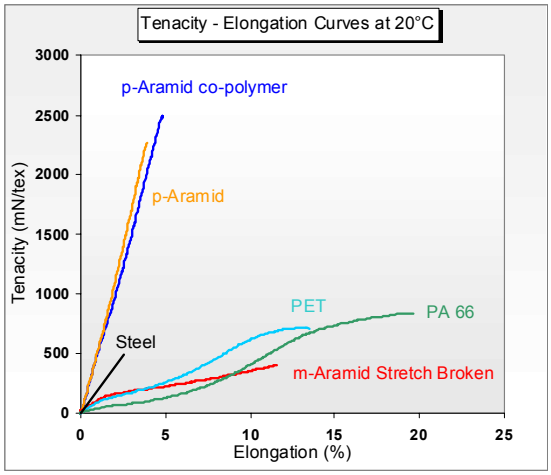

With aramid reinforcement it is possible to make many high performance automotive rubber parts:

1. radiator hoses – must withstand severe loads and conditions like heat, automotive fluids on the in- and outside, pressure and vibrations. Using aramid fibre reinforcement in knitted form gives large freedom of design for radiator hoses that withstand these severe conditions.
2. turbo hoses – these face even tougher conditions on tem-

perature, pressure and vibrations/dynamic loads. Aramids have an excellent track record in turbo hoses. They are especially suited for the next generation turbos with increased operating temperatures.

3. transmission-belts – these transfer strong, dynamic forces. Working life is much extended with aramid fibre as they have high modulus, strength and reduce belt abrasion. Belts and pulleys can be constructed smaller to save weight and space.
4. tires – need low weight reinforcement that is both flexible to withstand the continuous change of shape of rolling tires and strength and stiffness for predictable deformation and force transfer.
5. low rolling resistance tires – with chemically modified aramid short fibres, the heat build up in a filled rubber is significantly reduced, leading to substantially lower fuel consumption, longer life and lower wear.

The car industry in Central & Eastern Europe is looking for suppliers close to its plants. Using aramids to develop and manufacture high performance rubber products offers superb chances for local producers to supply to the automotive industry.

CL-11
STRUCTURE AND PROPERTIES OF POLYESTER FIBERS FROM DMT AND TEREPHTHALIC ACID FOR RUBBER INDUSTRY

M. JAMBRICH[a], J. ROSA[b], O. JAČANIN[b], K. ŠČASNÍKOVÁ[a], and M. BEČAVEROVÁ[a]

[a] *Faculty of Industrial Technologies, TnU AD Púchov,*
[b] *Kordtrade, s.r.o. Senica*

The work is aimed at preparation and evaluation of structure and basic utility properties of high-modulus, low-shrinkage polyester technical fibers prepared from different initial raw materials, DMT and terephthalic acid (PTA), produced by continuous spin-draw process. The evaluation of PET technical fibers was centered on physical-mechanical properties and on supramolecular, morphological, and macromorphological structure parameters. The results of the comparison of properties and structure of fibers have confirmed that fibers made from terephthalic acid represent a more favorable type of technical polyester fibers.

Introduction

High-tenacity polyester fibers have been marketed since the 1960s and have become the dominant construction material for various technical applications. PES technical fibers include conventional high-tenacity types (HT), as well as high-modulus low-shrinkage types (HMLS). HMLS fibers have higher dimensional stability and are preferentially used for the production of tires. The development of HMLS fibers was influenced mostly by increased requirements of the rubber industry. Main suppliers of PES fibers include global corporations, such as AKZO (now ACORDIS) KoSa (former Hoechst Celanese), Honeywell (as a part of General Electric), and Kordtrade[1].

Polyester technical fibers are used in a wide range of applications in automotive and rubber industry and for the production of various composite construction materials. Today's advanced technologies of preparation importantly increase the level of usage of PES technical fibers[2–4,7].

In the future, the automotive industry, as well as other sectors will need to develop newer fibrous materials with better utility properties. Today, the world production of PES cord is more than 300,000 t/y.

Leading production companies have developed special technologies of its preparation based on production of high-molecular PES polymers spinned at high speeds. HMLS PES fibers differ from conventional types by their supramolecular and morphological structure and corresponding thermodynamic-mechanical properties.

Experimental part

Experimental works were focused on the preparation of PES technical fibers type HMLS from DMT and terephthalic acid with linear density of 1,500 dtex by means of continuous process, and on the evaluation of their structure and utility properties. In polymers used to produce HMLS fibers from DMT and terephthalic acid, the viscosity limit number LVČ was > 100 mL g^{-1}. The preparation of fibers was carried out on a continuous equipment at Vn > 6,000 m min^{-1} (Fig. 1).

Prepared technical polyester fibers were evaluated for their supramolecular structure parameters (Δn, speed of sound – C, crystalline portion – β), mechanical properties (tenacity, elongation, E, shrinkage), and thermodynamic-mechanical properties (tg δ = E“/E’) at temperatures from −50 to 250 °C (ref.[5,8]).

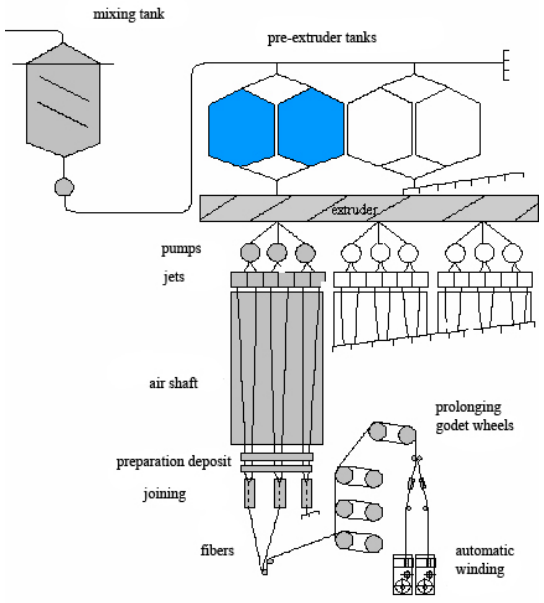

Fig. 1. **Diagram of the equipment for continuous preparation of PET fibers**

Thermodynamic properties parameter tg δ (E“/E’ = level of mechanical losses) is displayed on Fig. 2, 3.

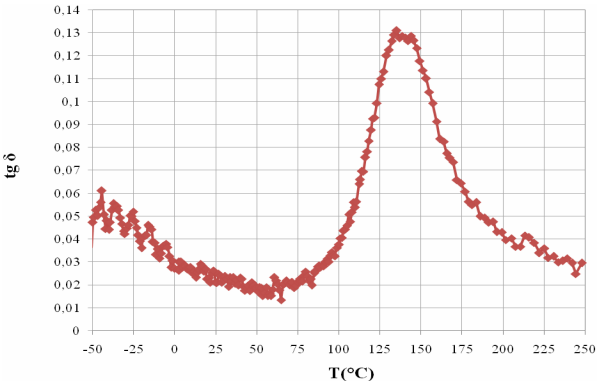

Fig. 2. **Loss factor tg δ of fibers from DMT fibers**

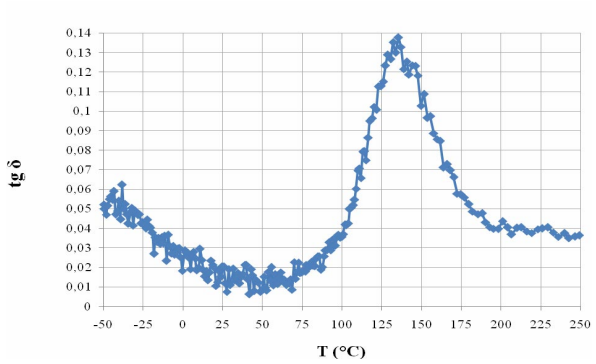

Fig. 3. **Loss factor tg δ of fibers from PTA fibers**

Discussion and conclusion

Our work was aimed at preparation and evaluation of physical-mechanical properties, supramolecular, morphological, and macromorphological structure parameters, and dynamic-mechanical properties of PET technical fibers from dimethyl terephthalate and terephthalic acid. Fibers were prepared using a spin-draw equipment. Based on obtained results from the evaluation of physical-mechanical properties, thermodynamic properties and structure parameters, we suggest the following conclusions:

Physical-mechanical properties (tenacity, elongation) and shrinkage of polyester HMLS fibers prepared from DMT and terephthalic acid (PTA) are comparable, but the tenacity is partly higher in fibers from terephthalic acid.

The comparison of module LASE, thermodynamic-mechanical properties and loss angle tg δ showed that the fibers prepared from terephthalic acid are more suitable.

Morphological and macromorphological structure of polyester fibers prepared from DMT and terephthalic acid are essentially on the same level, with high homogeneity and uniformity of inner structure and transversal geometry.

Supramolecular structure parameters (orientation and crystalline portion) suggest that the polyester fiber prepared from terephthalic acid has partly higher average orientation and crystalline portion, which results in more favorable physical-mechanical properties.

We can state that the properties of polyester HMLS fibers prepared from DMT and PTA are in accordance with the criteria for PET fibers applied in technical textiles.

REFERENCES

1. Wiliams L. Q.: International Fiber Journal. Polyester for Technical Textiles: Meeting Demands of Chalenging Market. *16*, 24 (2001).
2. Fourné F.: *Synthetic Fibers*. Hanser Publisherrs, Munich 1999.
3. Horrocks A. R., Anand S. C.: *The Textile Institute*. Woodhedsd Publishing Limited, Cambridge 2000.
4. Jambrich M., Budzák D., Kochan.J., in: prednáška na *59. Zjazde chemikov, 2.-6. september 2007, Vysoké Tatry, Tatranské Matliare* CD, Zborník, ChemZi 1/3, pp. 256−257 (2007).
5. Jambrich M., Pikler A., Diačik J.: *Fyzika vlákien*, Alfa, Bratislava 1987.
6. Jambrich M., Starigazda J., Sýkorová J., Cuninková J., Lániová A., in: prednáška na medzinárodnej konferencii *Slovak Rubber Conference, máj 2006, Púchov*, zborník.
7. Horrocks A. R.: *Handbook of Technical Textiles*. Woodhead Publishing Ltd, Cambridge 2000.
8. Bečaverová M.: *Diplomová práca*. FPT TnUAD, Púchov 2008.

CL-12
APPLICATION OF POLYMER NANOCOMPOSITES IN AUTOMOTIVE: THE PRESENT STATE AND PERSPECTIVES

VIERA KHUNOVÁ[a], IVAN KELNAR[b], and JÁNOS KRISTOF[c]

[a] The Slovak University of Technology, Faculty of Chemical and Food Technology, Institute of Polymer Materials, Radlinského 9, 812 37 Bratislava, SK, [b] Institute of Macromolecular Chemistry, Academy of Sciences of the Czech Republic, Heyrovsky Sq. 2, 162 06 Prague, CR, [c] University of Pannonia, Department of Analytical Chemistry, Egyetem 10, H-8200 Veszprém, HU

From point of view of application of polymer nanocomposites in automotive industry, the most significant fact is that together with remarkable improvement of end-use properties, the density of nanocomposites is virtually the same as that of the unfilled polymer. This means that substantial reduction of fuel consumption and air pollution, better performance and energy saving can also be made. According to a recent prognoses, widespread utilization of polymer nanocomposites in automotive would save annually over 1.5 billion liters of gasoline and would reduce carbon dioxide emissions by nearly 10 billion pounds[1].

Polymer nanocomposites often exhibit remarkable improvement in a wide range of physical and engineering properties:

- improved mechanical properties,
- reduced weight at the same performance,
- increased dimensional stability,
- improved barrier properties,
- increased heat distortion temperature,
- flame retardant properties (safety),
- high chemical resistance,
- high scratch resistance, smooth surface,
- electroconductivity,
- transparency (better visual impact).

The most stimulating for further development of polymer nanocomposites is the fact, that above property improvements are accessible in filler content which is about 10 times lower than currently used traditional fiber reinforced composites.

Althought the idea behind nanotechnology originated from Nobel Prize Laureate Richard Feynman 50 years ago, it took nearly 25 years, before the first polymer nanocomposite was prepared. The history of commercially used polymer nanocomposites has been written in 1989, when Toyota Motors introduced the first nanocomposites based on nylon 6 and clay (exfoliated montmorillonite). By replacing existing timing-belt cover material with PA6 nanocomposites they achieved together with high rigidity, no wrap, excellent thermal stability and the weight saving up to 25 %.

In spite of very optimistic prognoses, it took fairly long time untill other automotive companies followed Toyota and integrated polymer nanocomposites in their cars. The most recognized examples are summarized in the Table I.

It is now suggested that polymer/clay nanocomposites can be successfully applied in a range of vehicles for external and internal parts such as engine cover, oil reservoir tank, fuel hose, mirror housings, door handles and under-the-hood parts. Examples of current applications of polymer nanocomposites are given in Table II. It is believed that the weight advantage could bring except of significant environmental advantages also improvement in material recycling of used cars. That is why automotive is expected to be the second-largest application of polymer nanocomposites.

According the data[3] the volume of nanocomposites is expected to grow from $75 million globally market (in 2005) to $250 million in 2010[3]. Even more optimistic prognoses are given by Freedonia analyses[4]. They expext that by 2010, nanocomposites demand will grow to over $ 273 million, will further rise to over $3,8 billion in 2015 and $15 billion by 2020.

However, current economic crisis will certainly have its impact on the long term prognoses. For a while, automotive industry will very likely become reluctant to do major investments in innovative materials, thus certain delay in commercialization of new materials can be expected. On the other hand, the present situation in car industry may also be an opportunity for breakthrough innovations.

In spite the attractive properties and optimistic prognoses polymer nanocomposites applications are still far from to compete the market of high performance glass and carbon fibre reinforced composites. There are several reasons why commercialization of polymer nanocomposites is below the previous expectations.

Expect of difficulties connected with production of polymer nanocomposites in melt (only industrially acceptable mode), the second important reason is also lack of commercially available organoclays with acceptable thermal stability. This is because of most commercially available organoclays and nanocomposites (Table III, IV) are produced by the exchange of metal cations in clay galleries with thermally unstable organic ammonium salts[4]. Manufacturing costs also remain a significant factor restricting the growth of polymer–nanocomposite applications[4].

Table I
Concise history of polymer nanocomposites in car industry

Year	Company	Application
1989	Toyota Motors	Timing belt cover
	Mitsubishi´sGDI	engine cover
2004	General Motors	step assistant in GMC Safari and Chevrolet Astro vans, heavy-duty electrical enclosure
2006	Noble Polymer Forte PP	seat backs of Acura TL and center console of light truck.
2007	Yamaha Motor Corporation	light, smooth finish, nimble watercraft hulls made from NanoXcel

Table II
Current applications of polymer nanocomposites in automotives

Nanocomposite	Application
PA/clay	timing belt cover, car interior under hood
PP/clay	variety of applications replacing PP/talc and PP/glass fibres composites
TPO/clay	exterior car parts
PU/clay	car tyres
PP/clay	car body parts

Table III
Selected commercial nanoclays

Product	Producer
Nanomers	Nanocor
Closite	Southern Clay Products
Bentone	Elementis Specialties
Masterbatches	PolyOne, Clariant, RTP
Nanofil	Sud-Chemie
Planomers	TNO

Our research in polymer nanocomposites is related to

- Polypropylene composites based on natural nanofibres. The main research effort is oriented on study of potential application of natural nanotube in polypropylene nano-

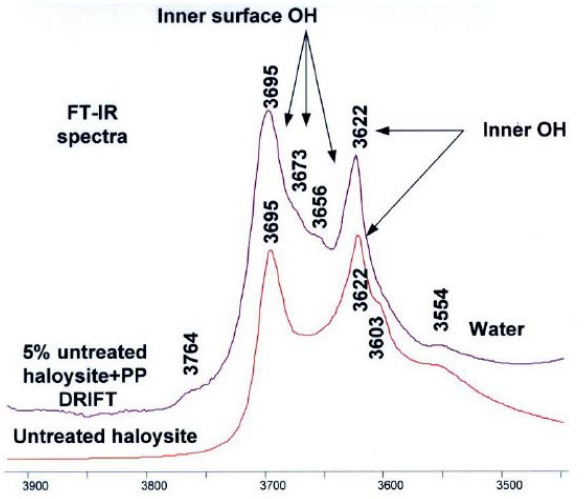

Fig. 1. **FT-IR spectra of hallosite and PP/halloysite composites**

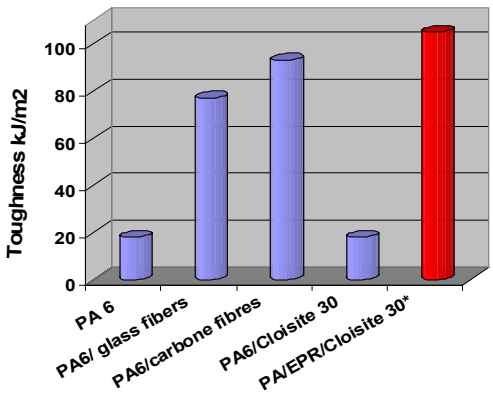

Fig. 3. **Comparison of toughness of short fibre (20 % w/w) and clay (5 % w/w) polyamide 6 composites**

composites

– Development of polyamide composites based on commercial organoclay and polyamide with improved toughness.

Comprehensive analyse of halloysite from source Michalovce Biela Hora, Slovakia has revealed that studied type of clay is favourable from both chemical structure (Fig. 1) and tubular particles (Fig. 2) for application in polymer nanocomposites. Our present work is focused on the development of effective and thermally stable modifiers as well as modification technologies enable to develop nanocomposites with improved end-use properties. The very first results indicate that an intensive intercalation of halloysite was achieved by mechanochemical treatment.

The impact of the intercalated structure of halloysite was confirmed by improving of mechanical properties, as well as reduction of flammability PP/halloysite nanocomposites. The investigation of structure of polymer nanocomposites based on intercalated halloysite confirmed considerable reduction of particle size and high degree of filler exfoliation.

Results related to our investigations concerning to polyamide nanocomposites are summarized in Fig. 3 and Table IV. It was found that by favorable combination of polyamide with EPR and two commercial organoclays with different polarity it is possible to prepare nanocomposites with highly (up to 400 %) improved toughness compared to neat polyamide without loosing stress, modulus and elongation.

This best balanced mechanical behaviour of PA6 nanocomposite was achieved by pre-blending of less polarity organoclay (Coisite 15A) into elastomer (EPR) followed by subsequent blending with PA and high polarity clay (Cloisite 30B). By this method a high degree of matrix reinforcement (exfoliation of clay with more polar treatment) was combined with favorable size and structure of dispersed EPR phase.

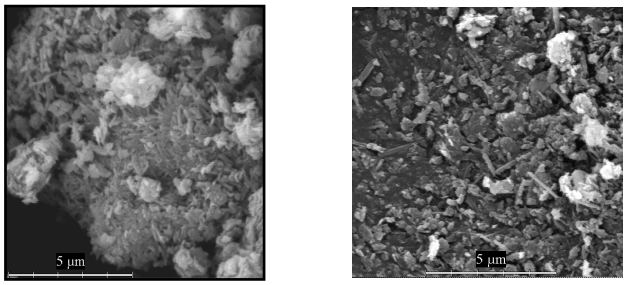

Fig. 2. **SEM analyse of Hallosite-Biela Hora, SK**

Table IV
Influence of glass fibres (GF), carbon fibres (CF) and organoclay (Cloisite 15, Cloisite 30) on toughness of PA6 composites

Sample	Filler content [% w/w]	Stress at break [MPa]	Elong [%]	E [MPa]
PA 6	0	74	150	1620
PA6/GF	20	138	7	3875
PA6/CF	20	151	5	7000
PA6/C30	5	94	90	2610
PA/EPR/C30	5	87	183	2560

The localization of less polarity organoclay in the interfacial area brought an important new effect consisting of enhancement of toughness by formation of “core-shell” particles. Detailed explanation of toughening effect is given in our papers[5,6].

Summary

In spite optimistic prognoses polymer nanocomposites applications present only negligible part and they are far from

to compete the market of currently used high performance fibre reinforced and particulate composites.

There are several reasons why commercialization of polymer nanocomposites in automotive is lower than the earlier prognoses. Among the key obstacles are:

- lack of commercial organoclay with acceptable thermal properties,
- difficulties related to structure of melt prepared nanocomposites,
- the extremely high price of carbon nanotubes.

Investigations related to polypropylene based on natural nanofibres underline the potential for future utilisation of halloysite from source Biela Hora, Slovakia, for production of polymer nanocomposites with outstanding end use properties.

It was found that by favorable combination of EPR and organoclays with different polarity it is possible to prepare nanocomposites with highly (up to 400 %) improved toughness compared to neat polyamide without loosing stress, modulus and elongation.

The project N°. 1/0662/08 was supported by Slovak Scientific Grant Agency (VEGA).

REFERENCES

1. MRS Report, 2003.
2. Zeng Q. H., Yu A. B., Lu G. Q. (Max), Paul D. R.: J. Nanosci. Nanotech. *5*, 1574 (2005). Markarian J.: Plastics *7*, 18 (2005).
3. *The Fredonia Group, Nanomaterials Demand in Composites*, Nanocomposites, Industry Study with Forecasts to 2010, 2015 & 2020, 2006
4. Pavlidoua S., Papaspyridesb C. D.: A review on polymer–layered silicate nanocomposites Progress in Polymer Science *33*, 1119 (2008).
5. Kelnar I., Khunová V., Kotek J., Kaprálková L.: Polymer *48*, 5332 (2007).
6. Khunová V., Kelnar I., Lehocký P.: The influence of interphase modifier on strucutre and properties of particulate and fibers polypropylene and polyamide composites, in proceedings of conference *Theplac, Brindisi, 2007*.

CL-13
WASTE OF POLYAMIDE 6.6 FLOCK FROM AUTOMOTIVE INDUSTRY AS A FILLER OF POLYAMIDE 6 COMPOSITE

KORNIEJENKO KINGA and KUCIEL STANISLAV

Cracow University of Technology (Poitechnika Krakowska), Al. Jana Pawła II 37, Kraków, Poland
kkorniej@wp.pl

Polyamide 6.6 flock is used as a material for aluminum gaskets during their production. The powder is atomized on gaskets and covers the surface, the rest of the powder is treated as a waste. Every month several tones were created and the company had to pay for their utilization.

In order to appraise the potential possibilities of use there were made some tests on the powder from the waste production. The possibility of material recycling was evaluated.

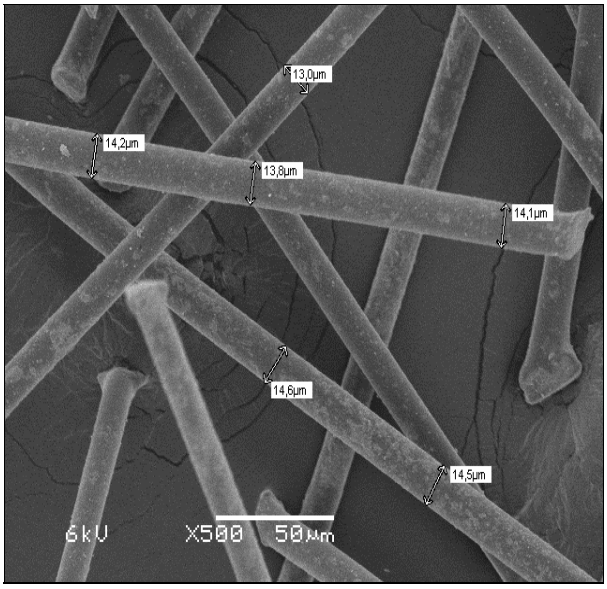

Fig. **Photography 1. SEM** – waste of flock

The waste of flock is for the most part homogeneous and little dirty or glutted. Flock, in its physical form, is fibers of polyamide 6.6 a length of 500 μm and the average diameter of 14–15 μm.

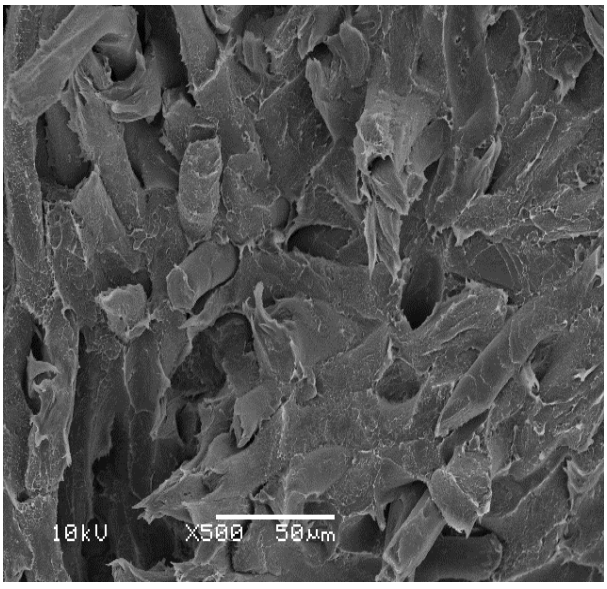

Fig. **SEM image of cross section after elongation test** - composite 4PA – polyamide 6 filled by 40% of waste flock

It is possible to use a flock as a filler to composite – by mixing it with the standard granuled Polyamide 6. After the preliminary trials rejected the possibility of direct injection flock, because of the difficulty in collecting the material, and

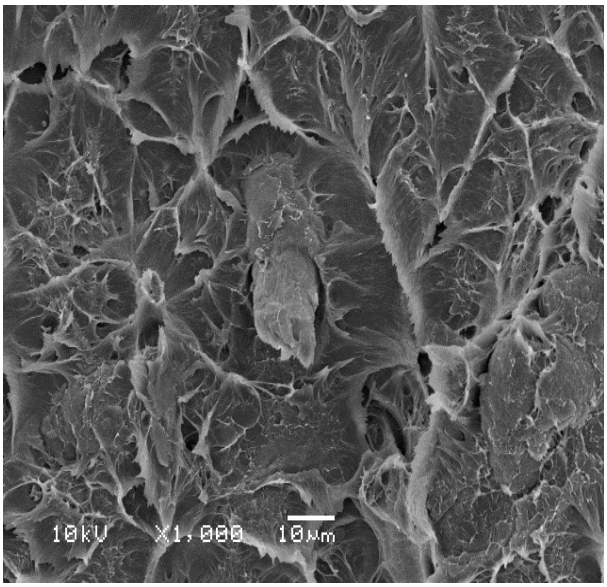

Fig. **SEM image of cross section after elongation test** - composite 2PA polyamide 6 filled by 20% of waste flock – simple flock fiber on the base of PA6 matrix

performed the test sample from two types of composition, from the compare used a samples from Polyamide 6.

Marker the samples used for testing:

PA6	–	Polyamide 6 – Tarnamide T27
2PA	–	20 % flock and 80 % T27
4PA	–	40 % flock and 60 % T27
PA6D	–	Polyamide 6 – Tarnamide T27 after 1 day washed a samples
2PAD	–	20 % flock and 80 % T27 after 1 day washed a samples
4PAD	–	40 % flock and 60 % T27 after 1 day washed a samples
PA6M	–	Polyamide 6 – Tarnamide T27 after 1 month washed a samples
2PAM	–	20 % flock and 80 % T27 po 30 after 1 month washed a samples
4PAM	–	40 % flock and 60 % T27 after 1 month washed a samples

Tested properties of tensile strength in the sample on a strength machine INSTRON: tensile strength, modulus of elasticity, strain at break for these 3 compositions and 3 states – dry samples in two weeks after injection, drenched samples after 1 day and 1 month. We can see a reduction in absorbance of water after adding the flock to pure PA6.

Results for determining the mechanical properties were compared which is reveal below:

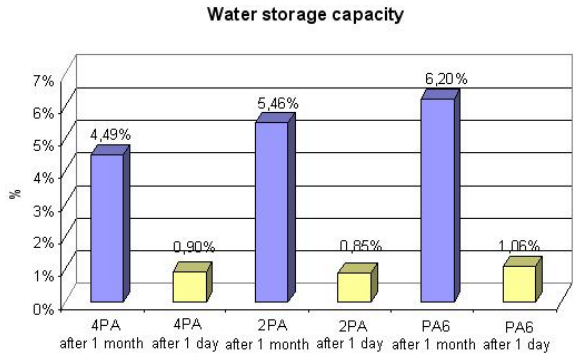

Chart 1. **Compare a water absorption samples with different additive material waste**

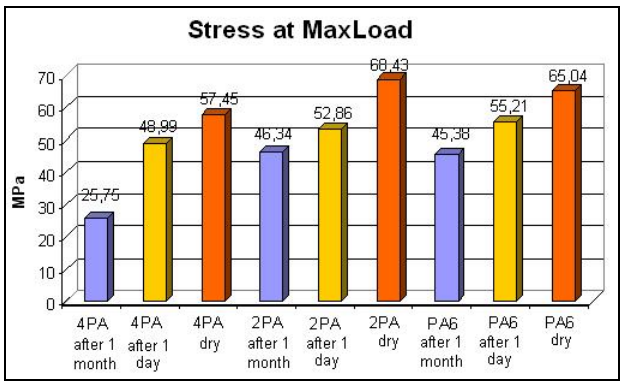

Chart 2. **Stress at MaxLoad**

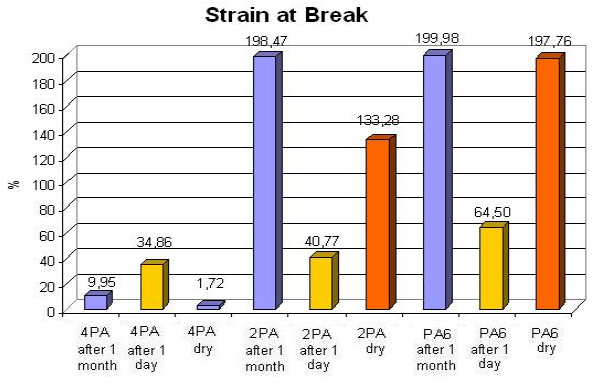

Chart 3. **Strain at Break**

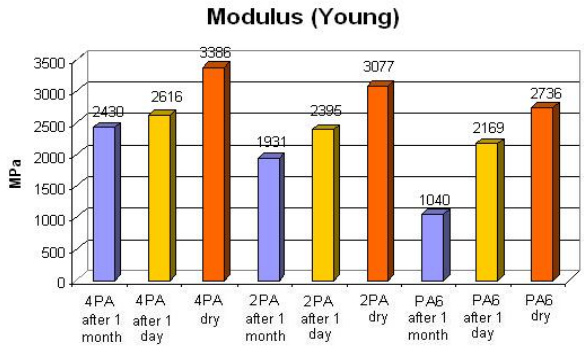

Chart 4. **Modulus (Young)**

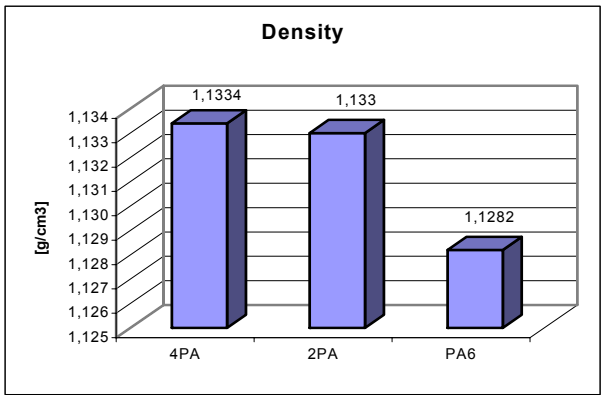

Chart 5. **Density**

Summing up the possibility of using flock by recycling material we can say that it appears to be the optimal use of the flock as a 20 % addition to polyamide 6 (for example Tarnamide T27). 20 % additional waste of flock can develop an increase of about 20 MPa modules of elasticity and slight decrease in strain at break. In this case it is also important to reduce absorbance of water in this composition.

Conclusion

The flock can be used as a supplement to original polyamides (black colored) or others materials.

It appears to be the optimal use of the flock as a 20 % addition to polyamide 6.

CL-14
EXPERIMENTAL RESULTS IN STABILIZATION OF STYRENE- BUTADIENE RUBBER

K. KOSÁR[a], P. LEHOCKÝ[a], P. ŠIMON[b], J. UHLÁR[a], and M. ĎURAČKA[a]

[a] VUCHT a.s. , Nobelova 34, 836 03 Bratislava, Slovakia,
[b] Slovak Technical University, Faculty of and Food Chemical Technology,Departmen of Physical Chemistry, Radlinského 10, 812 37 Bratislava, Slovakia
kkosar@vucht.sk; peter.simon@stuba.sk

The presentation deals with the stabilization of synthetic rubbers before their processing by the consumers. It shows the used methods of evaluation of the stability of rubbers during thermo-oxidative and thermo-mechanical duration and also gives real results from comparing measurements of efficiency of different types of stabilizers during stabilization of emulsion type SBR.

CL-15
MAGNETIC ELASTOMERIC MATERIALS FOR INTELLIGENT TYRES

J. KRUŽELÁK, R. SZABOVÁ, D. BELLUŠOVÁ, G. KYSELÁ, and I. HUDEC

Slovak University of Technology in Bratislava, Faculty of Chemical and Food Technology, Institute of Polymer Materials, Department of Plastics and Rubber, Radlinského 9, 812 37 Bratislava, jan.kruzelak@stuba.sk

Tyres are one of the most extensive and economic effective products of rubber industry. The demands on their driving properties increase with increasing of running speed and transport safety of modern vehicles. The progress in this sphere is also aimed at intelligent tyres that are able to respond to changes of driving conditions. One of possibilities of their construction is application of magnetic materials. They can be applied as permanent magnets able to communicate with external sensors[1,2]. The rubber compounds filled with powdery magnetic fillers are possible to include among these materials. They can be used to produce tyre sidewalls or treads, eventually small rubber components incorporated in tyres. The study of the change of elastomeric magnetic material properties in model and real rubber systems is focus of this work as well.

In this work the two different types of rubber compounds were used. Model rubber compounds A based on natural rubber NR, besides rubber and fillers, contained only ingredients which support curing process. Strontium ferrite $SrFe_{12}O_{19}$ (F) type FD 8/24 together with carbon black (CB) type N-660 were applied as fillers. The total content of fillers was kept constant (60 phr), only the weight fraction of ferrite in the combination of both fillers (w_f = F/(F+CB)) was changed. In case of rubber compounds B, real rubber compound which is generally used for producing passenger tyre sidewalls was used. These rubber compounds based on three diene rubbers

of general purpose (SIR20-NR, SBR, SKD20-BR) contained combination of ferrite and carbon black as fillers as well.

The results of study of physical – mechanical properties of vulcanizates A showed that the combination of applied fillers affects especially moduli. From Fig. 1 is evident significant decrease of modulus M300 with increasing of ferrite loading in fillers combinations. The decrease of modulus value of vulcanizate filled only with ferrite represents at about 260 % in comparison with modulus value of vulcanizate filled only with carbon black. The tensile strength of vulcanizates gently increases in whole examined ferrite concentration range in contrast to moduli.

The character of dependences of all evaluated physical-mechanical properties of vulcanizates filled with combinations of ferrite and carbon black points out its additive effect in model compounds of natural rubber.

The magnetic characteristics, namely remanent magnetic induction B_r, maximum magnetic induction B_m and maximum magnetic polarization J_m show significant non-linear increasing tendency with increasing of ferrite content in fillers combinations.

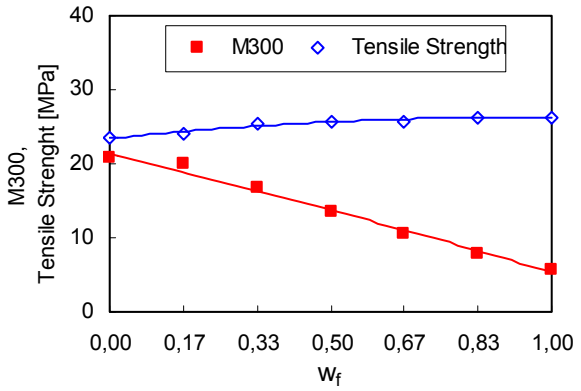

Fig. 1. **Influence of ferrite weight fraction w_f on modulus M300 and tensile strength of vulcanizates A**

Together, with the study of properties of elastomeric composites, the cross-link density and the sulfur cross-link structure were analysed. The highest total cross-link density ν_c exhibits vulcanizate filled with carbon black only and the lowest density ν_c vulcanizate filled with ferrite only. Therefore the increase of ferrite content in fillers combinations leads to consistent linear decrease of density ν_c. The chemical cross-link density ν_{ch} of all evaluated vulcanizates is lower than total cross-link density, but the differences between both densities become less with w_f increasing, above the $w_f > 0.5$ their values become nearly the same. The content of physical cross-links is low. With w_f increasing the next decrease of density ν_f was shown (Fig. 2). In the cross-link structure only polysulfidic and disulfidic cross-links were experimentally found with dominance of polysulfidic cross-links.

The study of influence of magnetic filler content on properties of real rubber compounds B was based on two-factor five-level planning experiment. As independent variables the weight ratio of ferrite and carbon black – x_1 (x_1=F/CB) and the total content of applied fillers in rubber compounds – x_2 (x_2=F+CB) were chosen. The content of carbon black was changed from around 15 phr to 54 phr and the total content of ferrite was changed from about 11 phr to 54 phr.

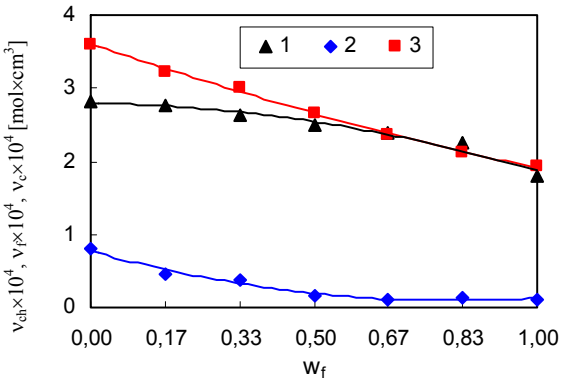

Fig. 2. **Influence of ferrite weight fraction w_f on chemical ν_{ch} (1), physical ν_f (2) and total cross-link density ν_c (3) of vulcanizates A**

The values of modulus M300 are relatively low and the differences between the modulus of vulcanizates filled with various ferrite content and various total content of both fillers are low as well. With increasing of weight ratio of both fillers F/CB the evaluated modulus non-linearly decreases. The increasing of total content of fillers F+CB has almost no influence on modulus M300 (Fig. 3).

The remanent magnetic induction shows a slight maximum with increasing of weight ratio of ferrite and carbon black. With increasing of total fillers content non-linear increasing tendency of observed magnetic property was detected. The increase becomes more evident with increasing of ferrite in combination of used fillers (Fig. 4).

The influence of magnetic filler content on cross-link density was evaluated on the chosen samples with different content of ferrite and carbon black. The results of measure-

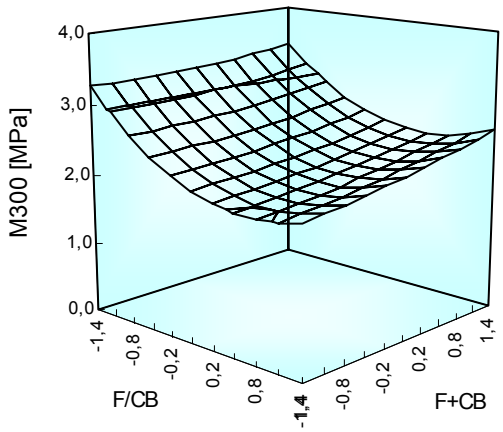

Fig. 3. **Influence of weight ratio of ferrite and carbon black (F/CB) and total content of fillers (F+CB) on M300 of vulcanizates B**

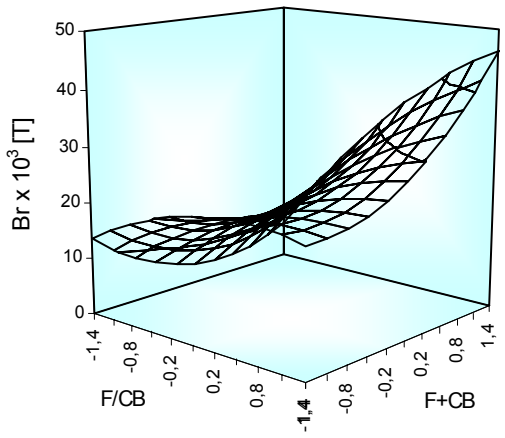

Fig. 4. **Influence of weight ratio of ferrite and carbon black (F/CB) and total content of fillers (F+CB) on remanent magnetic induction Br of vulcanizates B**

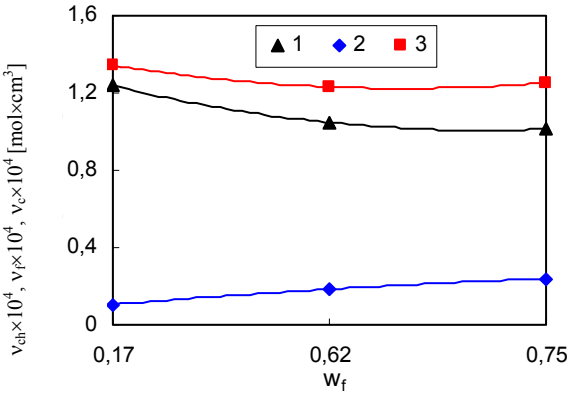

Fig. 5. **Influence of ferrite weight fraction w_f on chemical ν_{ch} (1), physical ν_f (2) and total cross-link density ν_c (3) of vulcanizates B**

ments showed, that the total cross-link density ν_c and the chemical cross-link density ν_{ch} gently decrease with increasing of ferrite loading in combination of both fillers. Despite of that the physical cross-link density ν_f is low as well as in case of vulcanizates A with w_f increasing slight increase of ν_f was observable (Fig. 5).

All types of sulfidic cross-links are present in prepared rubber compounds B with dominance of polysulfidic cross-links. The content of polysulfidic cross-links gently decreases with increasing of ferrite loading, while the content of dissulfidic cross-links gently increases with the same observed parameter.

REFERENCES

1. US Patent, US6550320 B1, April 22, 2003
2. Grönefeld M.: *Encyclopedia of Materials Science and Technology*, Permanent Magnets-Sensor applications, p. 6822–6825, 2003.

CL-16
WEAR OF MULTIPURPOSE TIRE TREADS

DAVID MANAS, MIROSLAV MANAS, MICHAL STANEK, MILAN ZALUDEK, STEPAN SANDA, JAKUB JAVORIK, and VLADIMIR PATA

Tomas Bata University, Faculty of Technology, Department of Production Engineering, TGM 275, 762 72 Zlin, Czech Republic
dmanas@ft.utb.cz

Abstract

Wear of tire treads at roads surfaces is measured as abrasion resistance. Off – road behavior of tire treads on surfaces with sharp stones is not well characterized by abrasion resistance as the mechanism of rubber damage is here rather different. The sharp edges of stones can cut a rubber tread surfaces and gradually tear off bigger pieces of rubber (chip – chunk).The aim of this article is evaluation of chip – chunk behaviour of different rubber compounds The process of the damage of multipurpose tire treads is described in this article as well.

Introduction

In rubber practice we often meet the problem of wear of the rubber parts. Some types of wear, especially the wear of tire treads, are very similar to machining. The tire tread (Fig. 1) is a part of tire that which in direct contact of the vehicle with the road and is thus is responsible for the driving force transfer. The wear of the tire tread of passenger and trucks cars travelling on common roads is characterized by its abrasion. The tread of a tire of a car is disposed to the abrasive effect of the road.

However, the mechanism of wear of tires working in very hard terrain conditions is absolutely different. Sharp stone edges and terrain irregularities gradually cut (tear off) parts of the rubber tread surface, which can be understood as a way of working – e.g. milling or turning, although under very specific conditions. The mechanism of tire tread wear working in hard terrain conditions is technically called Chip-Chunk effect and it can be considered as “workability” of

Fig. 1. **Cross section of radial tread of a passenger tire**, 1 – Inner-Liner, 2 - Carcass material, 3 – Bead wire (Core), 4 – Apex, 5 – Tire strip, 6 – Rim (Bead) strip, 7 – Sidewall, 8 – Breaker strip, 9 – PA Breaker strip, 10 – Tread

rubber surface.

The tire wear is usually tested under running conditions, these times demanding tests are very expensive. It would be very useful in practice to find a quick test of wear which could be carried out on small samples. Creating a model predicting the behavior of tire tread compounds would improve the development in wear research.

Experiment

Used materials (compounds)

Thirteen kinds of tire tread compounds used for motorcycle treads subjected to high stress, treads for technical, agricultural and multipurpose vehicles were experimented. All compounds represent real products and are produced and machined:

- Motorcycle tread cross (compounds number 183, 185, 186),
- Motorcycle tread enduro (compound 290),
- Technical vehicle treads (compound 188),
- Agricultural tire (104, 110, 114, 116),
- Gear tire (161),
- Tire for high-lift (162),
- Farm-tractor tire (165),
- MPT/R (168).

Test of wear

The tests of tire (tread) wear are time and money consuming. They are carried out using real tires in testing rooms or directly in the terrain during driving tests. That is one of the reasons for searching a method that would in a very short time (in minutes) and on small samples test the wear for a comparison of the different kinds of compounds.

Based on these requirements an equipment seen on Fig. 2 was designed. The Chip – Chunk wear testing machine (J. R. Beatty and B. J. Miksch in RCHT, vol. 55, p. 1531) was used for basal measurements. A new machine enabling changing the tested parameters and true simulations of the process conditions was designed, see Fig. 2.

Arm 1 pivotable around the neck is lifted by lifting part (piston of the pneumatic cylinder) 2. The arm that has a special ceramic edge tool is lifted and dropped 3 on the perimeter of the revolving wheel 4 (testing sample) driven by the electric motor 5. When it drops on the revolving wheel, the ceramic tool gradually chips the material and creates a groove on the wheel. The size of the groove chipped by the ceramic tool in a given time is the scale of wear. The following requirements had to be taken into consideration during the design:

- The rotations of the wheel (testing sample) must be adjustable in a wide range. To fulfill this requirement, an electro motor with adjustable revolutions using a static converter of frequency was chosen. This eliminated reduction of the revolutions by a transmitter enabling the frequency to be regulated from 0 to the maximum value. An electro motor 4AP80 – 6s and a static converter of frequency Alitivar 08 were used.
- For an adjustable arm lift a pneumatic mechanism composed of piston with adjustable lift was designed and machined. The cylinder is supplied directly from the regulated valve EVK 3120 by SMC and the process is controlled by a control unit FESTO type FEC – FC20/10W.
- Secure the constant parameters of the edge tool. First, a steel tool was designed, which however lead to a very fast wear changing the conditions of the experiment. For this reason a ceramic tool was tested – a treated edge for cutting tools (type TNGN 220608, Saint Gobein). Cutting edges with 60° angle were ground (Fig. 2).

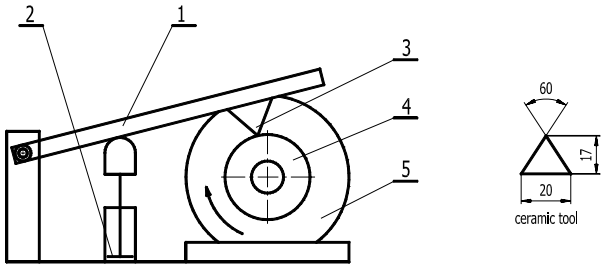

Fig. 2. **Design of testing equipment;** 1 – Arm, 2 – Pneumatic cylinder, 3 – Ceramic tool, 4 – Rubber sample, 5 – Electric motor

The ceramic edges proved a perfect resistance to wear. If the tool was well manipulated there was no difference between original and "worn" plate.

Dimensions of the testing sample

For easier preparation of testing samples the form seen on Fig. 3 was designed (the outer dimensions correspond to the testing sample of test Luepke).

A groove was made (chipped) by the ceramic tool into the testing sample during the experiment. It was expected

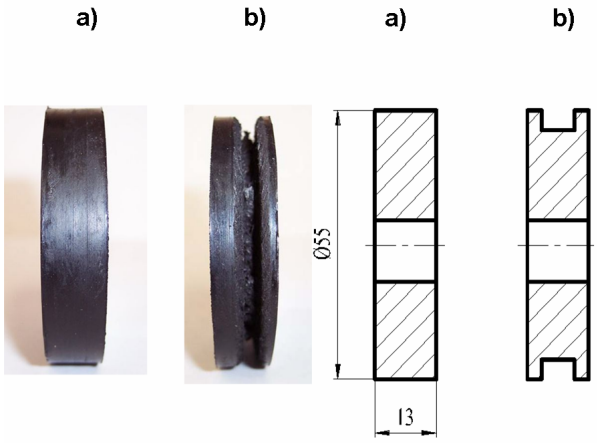

Fig. 3. **Testing sample for fast wear test a) before the test, b) after the test**

from experience with tooling other materials, esp. metals, wood or plastic, that the groove would be regular. Due to the properties of machined rubber – which demonstrated its elasticity – the moment the rotating ceramic tool dropped on the rotating wheel, pieces of material were torn off. For this reason, the initial intension of wear evaluation by measuring the groove diameter was changed to gravimetric evaluation.

Wear analysis

The influence of drop of the ceramic tool on the surface of the testing sample is crucial. If the sample were rigid, the evaluation of the impact of dropping force would be quite easy. The elastic properties of the testing sample however cause a series of other effects of smaller intensity (jumping on the surface) apart from the main effect (the first drop of the ceramic tool on the testing sample). The main effects of the ceramic tool have only partial influence on the total wear. It turned out that evaluating total work needed for wear (i.e. creating a groove on the testing sample) only by the energy of the drop would be biased. After the first testing of the experiment equipment, it was clear that the results in a given series of measurements would be comparable if the experiments ran under the same conditions. The construction of the main body with a key fitting the groove on the shaft and clamping basement with teeth prevent skidding of the testing sample while running and the control system of the testing machine will secure constant conditions for testing.

Test conditions

The conditions for experimental testing of fast wear were kept:

– Sample revolution 500 min^{-1}, 750 min^{-1}, 910 min^{-1}
– Impact frequency 1 Hz
– Ceramic tool stroke 60 mm
– Temperature 21 °C
– Test period 270s

The testing sample was clamped in the jaws of the machine to prevent is skidding and was rotated. The lifting mechanism for lifting the arm with ceramic tool was started. The time was measured from the first contact of the ceramic tool with the testing sample. Ten samples from each compound were used for the measurements. The mass loss was investigated by weighing on analytical balances after the experiment. Measured values were statistically evaluated.

The greatest wear was observed with compounds 183, 186 and 116. The best properties according to the wear were reported with testing samples prepared from compounds 168, 110 a 162 (Fig. 4).

Dependence on running conditions

The vehicles move in a different speed in the terrain in running conditions which can be characterised by the circumferencial speed of the tire tread. For this reason, other experiments were carried out to characterise the wear during different conditions. The wear test was done during the frequencies of testing samples of $n_1 = 910$ revolutions/min, $n_2 = 500$ revolutions/min, $n_3 = 250$ revolutions/min. The other conditions of the experiment remained unchanged. Fig. 5 shows the expected increasing tendency of the wear.

Wear procedure

The aim of the experiment was also to observe the mass difference of the testing sample (wear) during the test.

The mass of the samples was measured in regular inter-

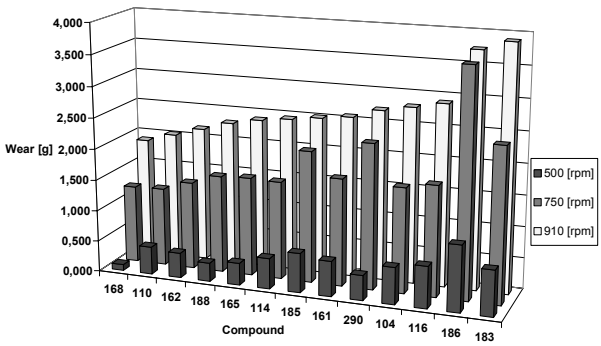

Fig. 5. **Comparison of mass loss at different frequencies**

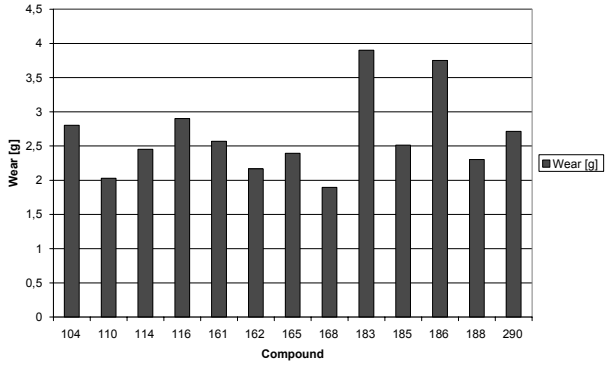

Fig. 4. **Comparison of the mass loss**

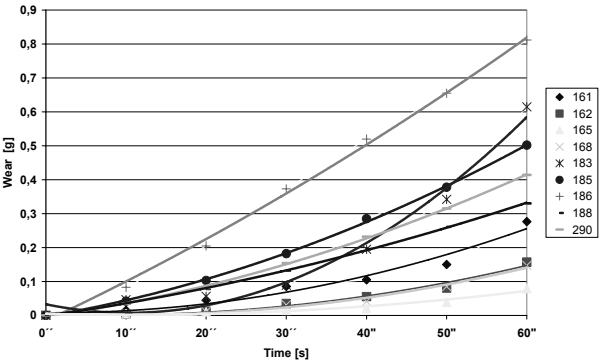

Fig. 6. **Gradual mass loss in all compounds in time 0–60 s**

vals (30 s) during the whole time of the experiment (270 s). Attention was paid to the interval 0–60 s due to the different behaviour of the tested compounds and the mass of the tested sample in this interval was measured every 10 s (Fig. 6, 7, 8).

Fig. 7. **Gradual mass loss in all compounds in time 0–60 s**

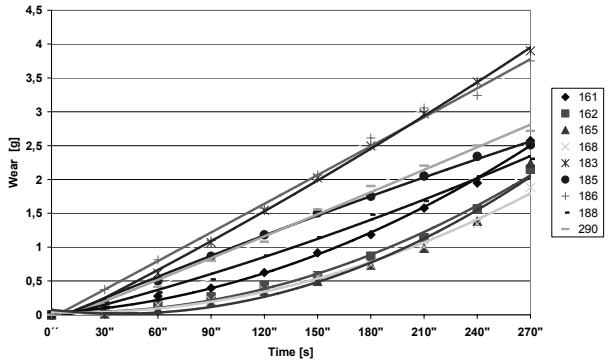

Fig. 8. **Gradual mass loss in all compounds in time 0–270 s**

Study of wear procedure using high speed camera

To be able to learn and understand much more the wear procedure the study using high speed camera was carried out. Observation of wear mechanisms showed that the wear mechanism itself happens in the area between the "splinter" and testing sample, which is found between already deformed and not yet deformed material. This is usually determined by the proportion between the layer thickness of the chipped rubber material and the thickness of the deformed "splinter". Considerable part of exerted energy (kinetic energy of the ceramic tool during drop) is – during the wear – concentrated to the place where the rubber material touches the ceramic tool and where parts of rubber material are detached.

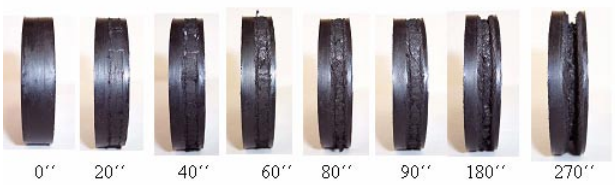

Fig. 9. **Wear of tested samples in time 0–270 s**

When investigating properties of the testing samples, high-speed video camera system Olympus i-SPEED 2 was used. The camera system was intended to visualize the behavior of the tested sample during the ceramic tool drop. The path of the ceramic tool when falling on the tested sample and the course of speed in a certain time were observed (Fig. 10, 11).

Discussion

The amount of the deforming force is closely related to the angle front (rake) of the ceramic tool (terrain roughness and sharp stone edges). In practice, this means that the angle front (rake) and the speed of motion on terrain roughness and sharp stone edges dramatically influence the conditions of created distortional deformation. The area between the splinter and rubber sample represents the crucial moment of the wear process during which material is taken away and splinter created. However, this is also a moment where shear stress and shear force, which have a substantial importance on the process happening on the ceramic tool area, are generated. Friction also plays a very important role, as the rubber material is during the ceramic tool drop exposed to high pressures. The rubber splinter is moving due to the deformation process on the front area of the ceramic tool and affects the temperature slightly by its activity and movement. There is a wide range of rubber mixtures with different properties. For that reason, it is necessary to pay attention to their behaviour and

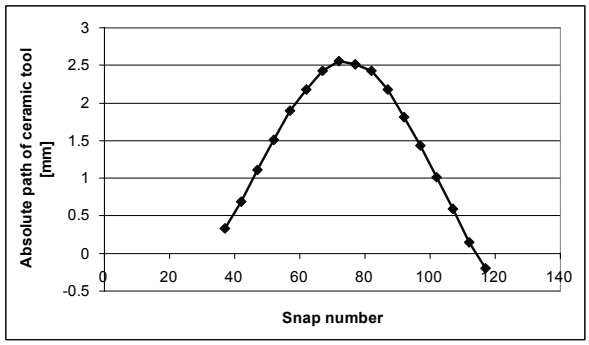

Fig. 10. **The absolute path of ceramic tool movement after dropping on the testing sample**

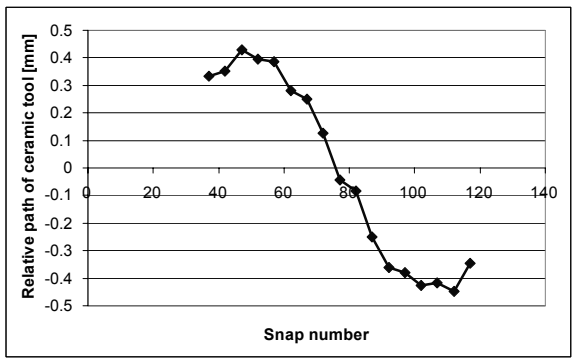

Fig. 11. **The relative path of ceramic tool movement after dropping on the testing sample**

bear in mind that the force ratio distribution during the wear is different with each mixture.

Conclusion

The presented test method shows the possibility of the evaluation of wear (chip – chunk) resistance of tire treads on small samples. This method makes possible to compare various types of compound with a standard and to observe the wear progress during the test period. The wear of the sample during the test period depends on the properties of rubber compounds and on test conditions.

The evaluation of the wear test using a high-speed video camera system Olympus i-SPEED 2 enables very detailed analysis of the wear process of heavily strained rubber parts, tire treads in particular. The visualisation of the ceramic tool drop on the testing samples can determine the path of tool penetration, as well as its speed (Fig. 10, 11). Simultaneously, the deformation of the testing sample can be observed. The path and speed ratio can determine the moment when the surface is damaged and first rips created.

This article is financially supported by the Czech Ministry of Education, Youth and Sports in the R&D project under the title 'Modelling and Control of Processing Procedures of Natural and Synthetic Polymers', No. MSM 7088352102.

REFERENCES

1. Batty J. R., Miksh B. J.: Rubber Chem. Technol. *55* (1989).
2. Johnson S. J.: *Rubber processing*, Hanser Publishers, Munich 2001.
3. Manas D.: *Rubber Workability and Wear of Rubber Parts*, VUT FSI, Brno 2005.
4. Manas D., Stanek M., Manas M., Dvorak Z.: *Off – Road Tires Behavior*, IRC 2005, Yokohama, Japan (2005).
6. ČSN ISO 37 Curred rubber or thermoplastic rubber – Tensile properties, Prague.

CL-17

SURFACE PROPERTIES OF POLY (IMIDE-CO-SILOXANE) BLOCK COPOLYMERS

IGOR NOVÁK[a]*, PETR SYSEL[b], IVAN CHODÁK[a], MILENA ŠPÍRKOVÁ[c], and IVICA JANIGOVÁ[a]

[a] *Polymer Institute, Slovak Academy of Sciences, 842 36 Bratislava, Slovakia,* [b] *Institute of Chemical Technology, Faculty of Chemical Technology, Dept Polymers, 166 28 Praha, Czech Republic,* [c] *Institute of Macromolecular Compounds of the Czech Academy of Sciences, 162 06 Praha, Czech Republic*
upolnovi@savba.sk

Abstract

Poly(imide-siloxane) (PIS) block copolymers have been studied with respect to their structure and surface properties relationship. The relatively small amount of siloxane in PIS block copolymer, 10–20 wt.%, increased significantly the contact angle of water due to the surface hydrophobization of the copolymer. The significant decrease of the surface energy of the PIS copolymer due to growth of the siloxane content was observed. The polar component of surface energy shows an intense decrease, whereas its dispersive component increases. The study of the morphology of PIS copolymers characterized by The X-ray Photoelectron Spectroscopy (XPS) analysis showed an excessive increase of Si on the polymeric surface. Scanning electron microscopy (SEM) shows a growth of the surface roughness by increase of the content of siloxane.

Introduction

Polyimides present a class of polymers, necessary in microelectronics, printed circuits construction, and aerospace investigation, mainly because their high thermal stability and good dielectric properties[1,2]. In the last years, several sorts of block polyimide based copolymers, namely poly(imide-siloxane) (PIS) block copolymers containing siloxane blocks in their polymer backbone have been investigated[3,4]. In comparison with homopolymer polyimides the PIS block copolymers possess some improvements, e.g. enhanced solubility, low moisture sorption, and their surface reaches the higher degree of hydrophobicity already at low content of polysiloxane in PIS copolymer. This kind of the block copolymers are used as high-performance adhesives and coatings. The surface properties of PIS block copolymers are strongly influenced by enrichment of the surface with siloxane segments. Micro phase separation of PIS block copolymers occurs due to the dissimilarity between the chemical structures of siloxane, and imide blocks even at relatively low lengths of the blocks. The imide segments at room temperature are below their glassy temperature and their mobility is reduced. The glassy temperature of siloxane segments is below the room temperature, thus these segments enable to migrate to the copolymer surface area.

Experimental

Synthesis of PIS block copolymers

2-Aminoterminated polyimides with controlled molecular weight were synthesized by solution imidization. The number-average molecular weights of products were in the range M_n = 2000–18,000 g mol^{-1} (by ^{1}H NMR spectroscopy). α,ω-bis(3-aminopropyl) polydimethylsiloxanes were prepared by anionic ring-opening equilibrium polymerization initiated with potassium siloxanolate. Their molecular weights were in the range M_n = 1000–5000 g mol^{-1}. Polyimide–polysiloxane copolymers were prepared via transimidization route[5].

Measurement methods

Surface energy

The surface energy of PIS block copolymer was determined via measurements of contact angles of a set of testing

liquids (i.e. re-distilled water, ethylene glycol, formamide, methylene iodide, 1-bromo naphthalene using SEE (Surface Energy Evaluation) system completed with a web camera (Masaryk University, Czech Republic). The surface energies of the polymer were evaluated by Owens-Wendt-Rabel-Kaelble (OWRK) equation modified by the least squares method[6].

XPS

The XPS spectra were recorded with an angle-resolved photoelectron spectrometer ADES 400 (VG Scientific) equipped with Mg Ka and Al Ka excitation sources, and a movable hemispherical electron energy analyzer. The analyzer was operated in the FAT mode at pass energy of 100 eV.

SEM

Morphology of the samples was studied by methods of electron microscopy – SEM and TEM. The surfaces of prepared block copolymers were observed using JSM 6400 (Jeol, Japan) microscope. The samples were sputter-coated by a thin layer of carbon due to better contrast of materials.

Results and discussion

Fig. 1 shows the surface energy ant its polar component of PIS block copolymer versus content of siloxane in copolymer. The surface energy of PIS decreases significantly with the concentration of siloxane from 46.0 mJ m^{-2} (net polyimide) to 34.2 mJ m^{-2} (PIS with 10 wt.% of siloxane), and to 30.2 mJ m^{-2} (PIS with 30 wt.% of siloxane). The polar component of the surface energy reached the value 22.4 mJ m^{-2} [net polyimide], which decreases with content of siloxane in PIS copolymer to 0.8 mJ m^{-2} (30 wt.% of siloxane) The decline of the surface energy, and its polar component of PIS block copolymer with raising siloxane content are very intense mainly between 0 and 10 wt.% of siloxane in copolymer. In the case of further increase of siloxane concentration (above 20 wt.% of siloxane), the surface energy of PIS copolymer, and its polar component is leveled off.

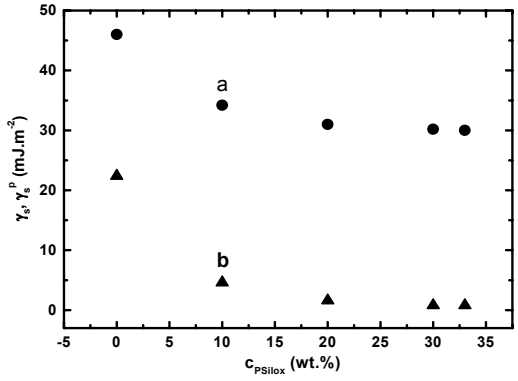

Fig. 1. **Surface energy (a) and its polar component (b) of PSI block copolymer *vs*. siloxane content**

XPS

Table I shows the element concentrations on the surface of the PSI block copolymer. For larger content of siloxane component, atomic concentration of Si increased, and atomic concentration of nitrogen decreased, as expected. XPS measurement was carried out at take-off angle of the emission 60˚ measured from the surface normal. The relation between Si and N reflecting the concentration of siloxane in PIS block copolymers is introduced to the last column of the Table I. The XPS results indicate the surface segregation of the siloxane component in the copolymer. The net polyimide contains by XPS analysis no Si atoms. XPS analysis at take-off angle 60° of PSI block copolymer shows an increase of the relation Si/N to: 6.8 (10 % copolymer); 19.6 (20 % copolymer). Only 2.8 of Si/N have been determined in the case of 30 % copolymer. The concentration of Si in 30 % copolymer is significantly lower than in the case of 20 % copolymers and might be caused by the changes in the chemical matrix of PIS block copolymer during its preparation. The above-summarized XPS results suggest significant enrichment of the surface layer of PSI block copolymer by Si and/or by siloxane segments most probably due to micro phase segregation the polar polyimide matrix.

SEM

Table I
Content of the element (at. %) at the surface of PSI block copolymers measured by XPS

	C	O	N	Si	Si/N
net PI	85.3	12.1	2.5	--	0
10 % silox.	73.5	14.9	1.5	10.2	6.8
20 % silox.	65.2	18.3	0.8	15.7	19.6
30 % silox.	81.9	12.2	1.6	4.4	2.8

SEM micrographs of net polyimide and PSI block copolymer with 30 wt.% of siloxane are shown in Fig. 2. The changes on the surface of the PSI block copolymers in comparison with net polyimide reflects the micro phase separation

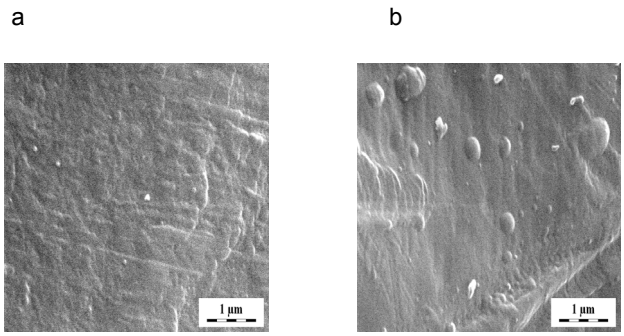

Fig. 2. **SEM micro photos of polymeric film containing net polyimide (a), and PSI block copolymer with 30 wt.% of siloxane (b)**

of the siloxane blocks forming a siloxane enriched circle places on the surface of the copolymer. SEM micrograph shows the surface of net polyimide (Fig. 2a) containing very fine roughness. In the case of 30 wt.% of siloxane in PSI copolymer (Fig. 2b) the roughness is higher comparing to net polyimide due to creation of the micro phase separated structure.

Conclusion

(i) the content of siloxane in copolymer increased, the surface energy, and its polar component of PSI copolymer diminished,
(ii) the morphology of PIS block copolymer has been changed due segregation of siloxane segments; constitution of polyimide continuous phase in copolymer was affirmed,
(iii) XPS analysis affirmed the surface segregation of the siloxane component in PIS copolymer.

The research was supported by Slovak Scientific Agency project VEGA, No. 2/7103/27 and by projects of the Grant Agency of the Academy of Sciences of the Czech Republic (A400500505, IAA100100622). and by Institutional Research Plan No. AV0Z10100521 is acknowledged as well.

REFERENCES

1. Chan-Park M. B., Tan S. S.: Int. J. Adhes**.** Adhesives *22*, 471 (2002).
2. Liaw W. C., Chen K. P.: J. Appl. Polym. Sci. *105*, 809 (2007).
3. Lu C., Wang Z., Liu F., Yan J., Gao L.: J. Appl. Polym. Sci. *100*, 124 (2006).
4. McGrath J. E., Dunson D. L., Mecham S. J., Hedrick J. L.: Adv. Polym. Sci. *140*, 61 (1999).
5. Sysel P., Hobzova R., Sindelar V., Brus J.: Polymer *42*, 10079 (2001).
6. Novák I., Števiar M., Chodák I., Krupa I., Nedelčev T., Špírková M., Chehimi M. M., Mosnáček J., Kleinová A.: Polym. Adv. Technol. *18*, 97 (2007).

CL-18
INVESTIGATION OF HIGH FREQUENCY DYNAMICS OF POLYMERS AND POLYMER BLENDS

CRISTIAN A. OPRISONI, THOMAS ALSHUTH, and ROBERT H. SCHUSTER

Deutsches Institut für Kautschuktechnologie e. V., Eupener Str. 33, 30519 Hannover, Germany
Cristian.Oprisoni@dikautschuk.de

A detailed knowledge of the dynamic – mechanical properties of elastomers on a frequency range that spans from 0,1–1 Hz to the high MHz region is highly awarded for modern product design. Currently, predictive testing of rubber parts at frequencies up to 1000 Hz can be performed with a reasonable accuracy by a wide array of testing equipments as for instance dynamic mechanical analyzers (DMA). Meanwhile, the behavior at higher frequencies, up to the MHz region, is affected by a scarcity of direct measuring techniques. The knowledge of the dynamic properties in this frequency range is crucially important for the prediction of grip phenomena.

The aim of this contribution is to study the influence different microstructures and fillers have on the high frequency dynamics of different rubbers. As a more global aim it is of great interest to predict the behavior of a rubber part during service when exposed to high frequency excitations.

The knowledge of the acoustic* properties of polymers, longitudinal and shear sound velocities and damping, contributes to a better understanding of the material properties at high frequencies especially of the structural characteristics of these polymers. The main characteristics of an acoustic wave are sound velocity and sound absorption or damping. The latter is a measure of the energy removed from the sound wave by conversion to heat during its propagation through a certain medium and it is a material property, different from attenuation, which also includes energy loss due to scattering and reflection and depends on sample size and experimental configuration.

Ivey et al. measured the longitudinal wave velocity and damping using the pulse transmission technique on IIR, SBR and NR at frequencies between 0.04 and 10 MHz in a temperature range from –60 °C to 40 °C. The rotating plate method was employed by Kono to measure transverse and longitudinal wave propagation on polystyrene and polymethyl methacrylate (PMMA) at frequencies of 0.5, 1 and 2.25 MHz in a temperature range from 20 °C to 210 °C and drew some conclusions with regard to the effect of large side groups on the positions of the longitudinal and shear maxima on the temperature scale and the effect of frequency on the maxima shift. Also Yee and Takemori calculated the dynamic compression modulus and the shear modulus from the simultaneous measurement of the dynamic Young's modulus and Poisson's ratio on PMMA at frequencies of 0.01, 0.1, 1 and 11 Hz between 0 °C and 40 °C.

Theoretical aspects

In an unbound, isotropic solid, two types of waves can be propagated. In one case the chain segments vibrate along the direction of propagation producing a longitudinal wave. In the other case the motion is perpendicular to the direction of propagation and is called a shear wave. The latter type of wave cannot be measured with the current experimental setup and will not be discussed here.

The current construction of the ultrasonic spectrometer allows the measurement of the longitudinal waves due to the positioning of the samples at a 90° angle to the incident wave.

* The term *acoustic* refers to a periodic pressure wave and it includes both audible and inaudible (infrasound and ultrasound) sound waves.

This position is critical since any variation of the angle would induce shear waves in the sample and reduce the precision of the measurement.

When longitudinal waves are propagated along thin strips and the wavelength is large compared to the sample thickness but small compared to its length the deformation is a simple extension and the complex Young's modulus is measured. At the other extreme, when the wavelength is small compared to the sample dimensions the wave propagation is governed by the complex longitudinal wave modulus:

$$M^* = M' + iM'' = \frac{4}{3}G^* + K^* \qquad (1)$$

where M* – complex longitudinal wave modulus, M' – storage part, M'' – loss part, G* – complex shear modulus, K* – compression modulus.
In the above equation the components of the complex longitudinal modulus are calculated as follows:

$$M' = \frac{\rho c_{rubber}^2 (1-\beta^2)}{(1+\beta^2)^2} \qquad (2)$$

$$M'' = \frac{2\rho c_{rubber}^2 \beta}{(1+\beta^2)^2} \qquad (3)$$

where

$$\beta = \frac{\alpha_{rubber} c_{rubber}}{2\pi f}$$

ρ – rubber density, c – sound velocity, α – damping coefficient, f – frequency

As can be seen from equations (*2*) and (*3*), the unknown terms are c_{rubber} and α, the sound velocity in the rubber and the attenuation coefficient, respectively. Both these terms are measured by the ultrasonic spectrometer (Fig. 1) and they give the first insight on the polymer behavior at high frequency.

As seen above calculating the components of the complex longitudinal wave modulus is not a difficult task, however comparing it with the complex shear modulus is quite tricky due to the composition of the first:

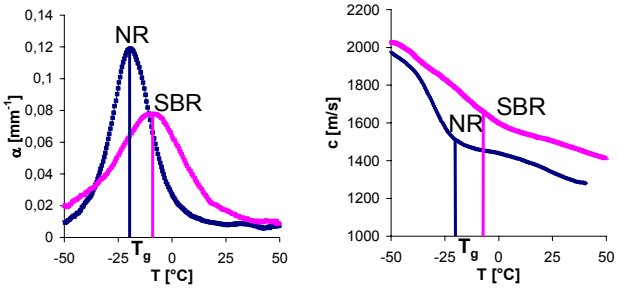

Fig. 1. **Sound attenuation (left) and velocity (right)**

$$M^* = \frac{4}{3}G^* + K^* \qquad (4)$$

$$K^* = K_0 + K_1^* \qquad (5)$$

$$K_1^* = K_1' + iK_1'' \qquad (6)$$

In the above equations K_1^* is the frequency dependent component and K_0 is the temperature dependent static compression modulus.

Experimental

The polymers used were, alongside the SBRs with varying styrene and vinyl content (Table I), SBR 2525, NR CV50 and 3 NBRs with different acrylonitrile (ACN) content (18, 28, 34 and 44 % ACN, respectively).

Table I
Solution SBR systems – styrene and vinyl variation

Material	SSBR 20/60	SSBR 20/45	SSBR 30/30	SSBR 20/30	SSBR 10/30
Styrene, %	21	21	30	21	10
Vinyl, %	62	46	33	31	33
T_g (DSC), °C	–21	–38	–38	–50	–60

The polymers were mixed and crosslinked to the rheometer optimum (160 °C) using a common vulcanizing system (sulfur – 2 phr, TBBS – 2 phr, stearic acid – 1 phr and zinc oxide – 3 phr) and an anti aging agent (6PPD) – 4 phr. Carbon black (N347) and silanized silica were incorporated at loadings of 20, 40 and 60 phr in an one step mixing process by using an internal mixer (Haake Rheomix 3000E) at 50 rpm.

Dynamic-mechanical analysis were carried out on samples of 2×10×35 mm^3 in size, on an RDA (Rheometrics Data Analyzer) apparatus, in torsion, at an amplitude of 0,5 %. The temperature increase rate for the temperature sweeps (–60 °C – +60 °C) was 1 °C min^{-1} and the testing frequency was 1 Hz.

High frequency measurements were performed in a prototype ultrasonic analyzer at 0,5 MHz using the wave transmission technique.

Results

Unfilled polymers

The increase of the styrene and vinyl content determines higher values of the loss moduli (Fig. 2).

The glass transition is shifted to higher temperatures with increasing styrene and vinyl content. This increase is

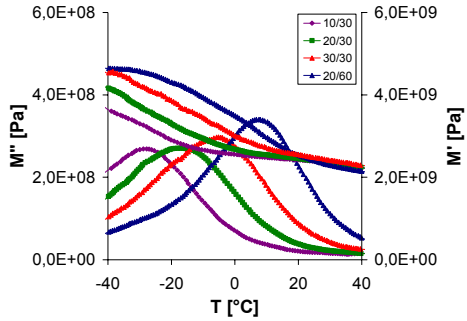

Fig. 2. **Real (M') and imaginary (M") part of the longitudinal wave modulus for unfilled polymers**

expected since the presence of side groups on a macromolecular chain induces steric hindrances that reduce its capability of free motion. Furthermore, the more side groups the more energy is needed for the chain to move and, hence, the higher the maximum of the M" peak.

It's worth noticing that the styrene influence, in the case of the SBRs, is lower than that of the vinyl due, probably, to an increased molecular friction induced by the latter.

A similar behavior is observed for NBR when increasing the ACN content. It brings about a shift of the glass transition to higher temperatures as well as an increase of the magnitude of the loss modulus. The NBR with the highest content of ACN also displays the smallest half width.

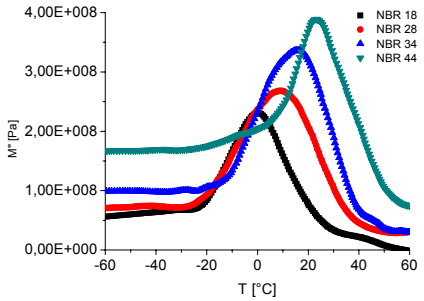

Fig. 3. **Loss component of the longitudinal wave modulus for unfilled NBRs with increasing ACN content**

Polymer blends (SBR:NR)

The discussion sets forth with the low frequency analysis. A first glimpse at the shear data ascertains that the two polymers are immiscible but for the SBR:NR 20:80.

A simple estimation shows that about 17 percent of the SBR is apparently soluble in the NR forming a single phase. Over this quantity, more SBR phase separation occurs with one pase composed of NR and SBR and a distinct second phase containing SBR only.

Table II
Glass transition temperature (G"max) of the SBR/NR blends

SBR/NR	0/100	20/80	40/60	50/50	60/40	80/20	100/0
Tg SBR, °C	n. a.	n. a.	–39	–41	–42	–42	–42
Tg NR, °C	–60	–58	–58	–58	–57	–57	n. a.

When one considers the glass transition temperatures of the different mixes, the addition of 20 percent of SBR induces a 2–3 °C shift in the transition temperature which does not change any further when adding more SBR. This shift compared to the 18 °C difference between the two raw polymers indicates an approximate amount of 15 percent of SBR in the mixed phase.

The 0,5 MHz measurements show the same ranking of the blends according to their different concentrations.

The difference between the transition temperatures of the 2 peaks is reduced from 18 °C at 1 Hz to only 14 °C at 0,5 MHz. The highest energy dissipation is shown by the unblended NR. With the addition of SBR the height decreases while the broadness of the peaks increases slightly. The glass transition temperature (due to the high frequency only one

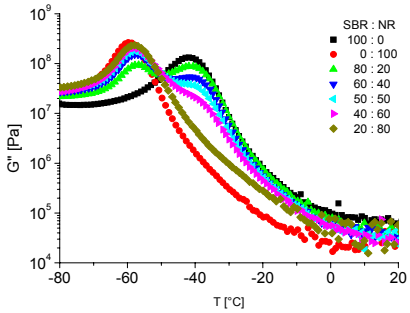

Fig. 4. **Shear modulus of the SBR/NR blends at 1 Hz**

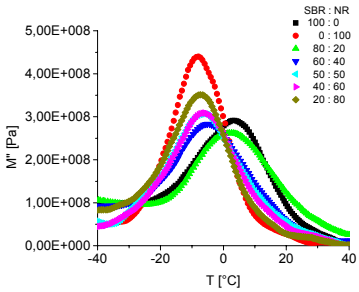

Fig. 5. **Energy dissipation of the SBR/NR blends at** 0,5 MHz

** The difference between the solubility parameters of NR (δ = ~1,7 $Pa^{-1/2}$) and SBR (δ = ~17 $MPa^{-1/2}$)[6] means that the two polymers are insoluble. However, the dynamic – mechanical measurement at 1 Hz does not distinguish 2 phases below 17 % of SBR

Table III
Glass transition temperature (maximum attenuation) of the SBR/NR blends

SBR/NR	0/ 100	20/ 80	40/ 60	50/ 50	60/ 40	80/ 20	100/ 0
Tg SBR, °C	n. a.	n. a.	n. a.	n. a.	3	4	6
Tg NR, °C	–8	–5	–5	–5	–4	–5	n. a.

peak is seen for all mixes) does not change significantly until 80 parts of SBR are added when it shifts close to the SBR temperature at 0,5 MHz. Seen from the right to the left, the addition of 20 parts of NR into SBR determines, similar to the addition of SBR in NR, a decrease in the maximum dissipated energy and a broadening of the peak. The joining closer together and the higher broadness of the peaks is a well known effect of the increase in frequency.

As a result the different peaks of the polymers can no longer be distinguished and the NR seems to dominate at this frequency.

Filled polymers

The addition of carbon black to the SBR mixes determines an overall increase of the moduli and a widening of the loss peaks due to the noticeable filler – polymer interaction.

As was to be expected the glass transition temperature does not vary significantly with the filler concentration.

Silica was also used in the experiments presented in this contribution. Because pure silica is seldom used nowadays, a surface treatment was applied using silan Si69. The silanization lead to important changes in its reinforcing characteristics. If one considers the surface energies of carbon black and (unsilanized) silica, the main difference resides in the fact that, due to its high dispersive component, carbon black achieves reinforcement by strong rubber-filler interactions while its filler-filler network is weak whereas silica reveals a weak interaction with the rubber (by comparison with carbon black) but a good interaction with itself forming a strong filler-filler network.

After the silanization, the dispersive component of the surface energies drops even compared to the unmodified silica, and the polar component (which gives a hint on the strength of the filler-filler interaction) becomes insignificant thus the formation of the filler network is prevented.

The result of this effect is shown in Fig. 7, where the maxima of the loss longitudinal modulus is plotted against the styrene fraction for unfilled rubber and filled with carbon black and silanized silica. The silica filled material displays lower energy dissipation than its carbon black filled counterpart.

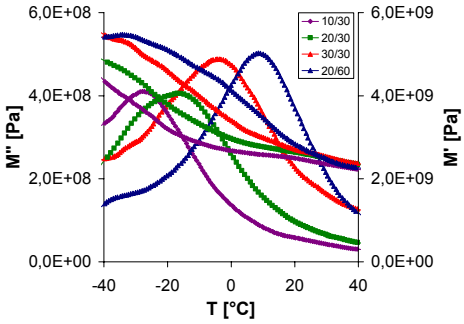

Fig. 6. **Real (M') and imaginary (M") part of the longitudinal wave modulus for filled polymers (60 phr carbon black)**

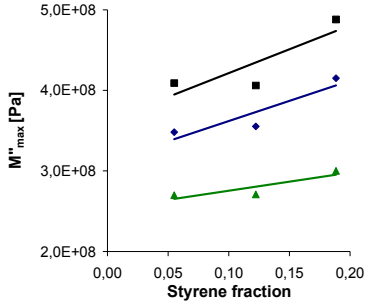

Fig. 7. **Filler and styrene content influence on the maxima of the longitudinal wave modulus**

Conclusions

A clear and accurate picture of the high frequency behavior of rubber materials is difficult to asses and ultrasound is one of the few methods able to directly measure dynamic properties in the MHz region.

The discrete influence of the polymer microstructure (vinyl, styrene and acrylonitrile content) as well as that of nanoscaled fillers on the chain dynamics is analyzed at 0,5 MHz.

Ultrasound spectroscopy proves to be a valuable tool in determining energy dissipation at high frequency for polymeric blends; the shifting procedure associated with the WLF equation cannot be applied to most blends.

The authors would like to express their gratitude to the Deutsche Kautschuk – Gesellschaft e. V. for providing the financial means to carry out this research and to Lanxess Deutschland GmbH and DOW Olefinverbund GmbH for supplying the polymers.

REFERENCES

1. Sinha M., Buckley D.: *Acoustic Properties of Polymers in Physical Properties of Polymers Handbook*, 2nd Edition, (J. E. Mark, ed.) *60*, 1021, 2007.
2. Ivey D. S., Mrowca B. A., Guth E.: J. Appl. Phys. *20*, 486, (1949).
3. Kono R.: J. Phys. Soc. Jpn. *15*, 718 (1960).
4. Yee A. F., Takemori M. T.: J. Pol. Sci., Part B: Polym. Phys. *20*, 205 (1982).
5. *Science and Technology of Rubber*, 2nd ed., Academic Press, 1994.
6. *Polymer Handbook*, Second Edition, J. Wiley & Sons, New York 1975.